European Journal of Pharmaceutics and Biopharmaceutics 75 (2010) 213–217

Contents lists available at ScienceDirect

European Journal of Pharmaceutics and Biopharmaceutics

journal homepage: www.elsevier.com/locate/ejpb

Research paper

Claudin-4-targeting of *diphtheria* toxin fragment A using a C-terminal fragment of *Clostridium perfringens* enterotoxin

Hideki Kakutani [a], Masuo Kondoh [a,*], Rie Saeki [a], Makiko Fujii [b], Yoshiteru Watanabe [b], Hiroyuki Mizuguchi [c,d], Kiyohito Yagi [a,*]

[a] Laboratory of Bio-Functional Molecular Chemistry, Graduate School of Pharmaceutical Sciences, Osaka University, Osaka, Japan
[b] Department of Pharmaceutics and Biopharmaceutics, Showa Pharmaceutical University, Tokyo, Japan
[c] Laboratory of Gene Transfer and Regulation, National Institute of Biomedical Innovation, Osaka, Japan
[d] Department of Biochemistry and Molecular Biology, Graduate School of Pharmaceutical Sciences, Osaka University, Osaka, Japan

ARTICLE INFO

Article history:
Received 30 October 2009
Accepted in revised form 4 March 2010
Available online 11 March 2010

Keywords:
Claudin
Targeting
Cancer
Diphtheria toxin
Clostridium perfringens enterotoxin

ABSTRACT

Claudin (CL)-4, a tight junction protein, is overexpressed in some human neoplasias, including ovarian, breast, pancreatic and prostate cancers. The targeting of CL-4 is a novel strategy for tumor therapy. We previously found that the C-terminal fragment of *Clostridium perfringens* enterotoxin (C-CPE) binds to CL-4. In the present study, we genetically prepared a novel CL-4-targeting molecule (DTA–C-CPE) by fusion of C-CPE and *diphtheria* toxin fragment A (DTA). Although DTA is not toxic to CL-4-expressing L cells, even at 20 μg/ml, DTA–C-CPE is toxic to CL-4-expressing L cells at 1 μg/ml. DTA–C-CPE-induced cytotoxicity was attenuated by pretreatment of the cells with C-CPE but not bovine serum albumin, indicating that DTA–C-CPE may bind to CL-4-expressing L cells through its C-CPE domain. To evaluate the specificity of DTA–C-CPE, we examined its cytotoxic effects in L cells that express CL-1, -2, -4 or -5. We found that DTA–C-CPE was toxic to only CL-4-expressing L cells. Thus, C-CPE may be a promising ligand for the development of cancer-targeting systems.

1. Introduction

Chemotherapeutic agents target the intracellular metabolic processes or growth rates that are different between malignant cells and normal cells, and rapidly growing cancer cells are sensitive to chemotherapies [1,2]. But, progressive cancer cells with a decreased growth rate respond poorly to chemotherapy [3]. Radiation therapy affects both the tumor and the surrounding normal tissue. These conventional therapies cause DNA damage, leading to genomic instability and susceptibility to neoplastic mutations [4]. Cancer cells often overexpress surface proteins, including growth factor receptors or antigens [5]; thus, targeting cancer cells by using the surface proteins is a promising strategy for cancer therapy. Ligands for growth factor receptors and cytokine receptors have been fused with fragments of bacterial toxins, such as *Pseudomonas* exotoxin and *diphtheria* toxin (DT) [3,6].

Tight junctions (TJs) form the apical junctional complex in epithelial cell sheets and play pivotal roles in the barrier of the epithelial cell sheets and the fence separating basal and apical components, such as receptors and transporters, on the membrane [7]. Epithelial TJs are dynamic structures that are modulated during neoplastic transformation [8]. The relationship between abnormal TJ function and epithelial tumor development has been suggested by earlier studies showing alterations in the TJ structures of epithelial cancers [9,10]. Loss of tight junction integrity may allow the diffusion of nutrients and other factors necessary for the survival and growth of the tumor cells [8]. Destruction of the fence function of TJs can lead to overproliferation of tumor cells [11,12]. If TJ components are exposed to the cell surface in cancer cells, they may be a promising target for cancer therapy.

Claudins (CLs) are key molecules in the formation of TJs; proteins in the 24-member claudin family contain four transmembrane domains [13]. CL-4 is frequently overexpressed in several neoplasias, including ovarian, breast, pancreatic and prostate cancers [12,14]. Thus, CL-4 may be useful as a target molecule in cancer therapy. CL-4 is a receptor for *Clostridium perfringens* enterotoxin (CPE), which is a single 35-kDa polypeptide that causes food poisoning in humans [15]. CPE exhibited anti-tumor activity

Abbreviations: C-CPE, the C-terminal fragment of *Clostridium perfringens* enterotoxin; DTA, *diphtheria* toxin fragment A; DTA–C-CPE, C-CPE-fused DTA; DT, *diphtheria* toxin; TJ, tight junction; CPE, *C. perfringens* enterotoxin; CL, claudin.

* Corresponding author. Laboratory of Bio-Functional Molecular Chemistry, Graduate School of Pharmaceutical Sciences, Osaka University, Osaka 565-0871, Japan. Tel.: +81 6 6879 8196; fax: +81 6879 8199 (M. Kondoh), tel.: +81 6 6879 8195; fax: +81 6879 8195 (K. Yagi).
E-mail addresses: masuo@phs.osaka-u.ac.jp (M. Kondoh), yagi@phs.osaka-u.ac.jp (K. Yagi).

0939-6411/$ - see front matter © 2010 Elsevier B.V. All rights reserved.
doi:10.1016/j.ejpb.2010.03.003

in CL-expressing cancers, such as breast [16], ovarian [17] and pancreatic cancers [18]. They did not observe side effects from CPE treatment, indicating that a ligand for CL-4 may be a promising candidate for cancer-targeting therapy.

CL has very low antigenicity, and there are few antibodies to the extracellular region of CL. CPE is composed of N-terminal cytotoxic domain and C-terminal receptor-binding domain [15]. C-CPE is the C-terminal receptor-binding domain, and C-CPE is the first CL-4-binder [19]. In the present study, we prepared a CL-targeting agent (DTA–C-CPE) consisting of C-CPE coupled to a protein synthesis inhibitory factor, fragment A of DT [20]. DTA–C-CPE had CL-4-specific cytotoxicity; thus, C-CPE may be a promising ligand for the development of cancer-targeting systems.

2. Materials and methods

2.1. Chemicals

Bovine serum albumin (BSA), 2-(2-methoxy-4-nitrophenyl)-3-(4-nitrophenyl)-5-(2, 4-disulfophenyl)-2H-tetrazolium (WST-8) and phosphatase inhibitor cocktail were purchased from Nacalai (Kyoto, Japan). Protease inhibitor cocktail and anti-β-actin mAb were obtained from Sigma–Aldrich (St. Louis, MO). Horseradish peroxidase (HRP)-labeled antibodies were obtained from Chemicon (Temecula, CA). Anti-His-tag antibody was purchased from Novagen (Madison, WI). All other reagents were of research grade.

2.2. Cell culture

L cells, a mouse fibroblast cell line, and mouse CL-expressing L cells were kindly provided by Dr. S. Tsukita (Kyoto University, Japan). Cells were cultured in modified Eagle's medium (MEM) supplemented with 10% fetal calf serum (FBS) at 37 °C.

2.3. Preparation of DTA–C-CPE

DTA (CRM45) cDNA was kindly provided by Dr. K. Kohno (Nara Institute of Science and Technology, Japan) [21]. The plasmids containing DTA fused with C-CPE were prepared as follows. DTA was amplified by polymerase chain reaction (PCR) with pTA–DTA as a template, a forward primer (5′-GCGGTACCATGGGCGCTGAT GATGTTGTTG-3′, *Kpn*I site is underlined) and a reverse primer (5′-CCTTAATTAATCGCCGTACGCGATTTCCTG-3′, *Pac*I site is underlined). The resulting PCR fragments were subcloned into *Kpn*I/*Pac*I-digested pETH$_{10}$PER (kindly provided by Dr. Y. Horiguchi, Osaka University, Japan), and the sequence was confirmed (pET–DTA–C-CPE). Double-stranded oligonucleotide of G/S linker was prepared by annealing (heating at 95 °C for 5 min and chilling at room temperature for 60 min) of single-strand oligonucleotides, a forward oligonucleotide (5′-TGGAGGAGGAGGATCTGGAGGAGGAGGA TCTGGAGGATACCCATACGACGTCCCAGACTACGCTAT-3′, *Pac*I site is underlined) and a reverse oligonucleotide (5′-AGCGTAGTCTGGGA CGTCGTATGGGTATCCTCCAGATCCTCCTCCTCCAGATCCTCCTCCTCCA AT-3′, *Pac*I site is underlined). The resulting oligonucleotides were subcloned into *Pac*I-digested pET–DTA–C-CPE, and the sequence was confirmed (pET–DTA-linker-C-CPE).

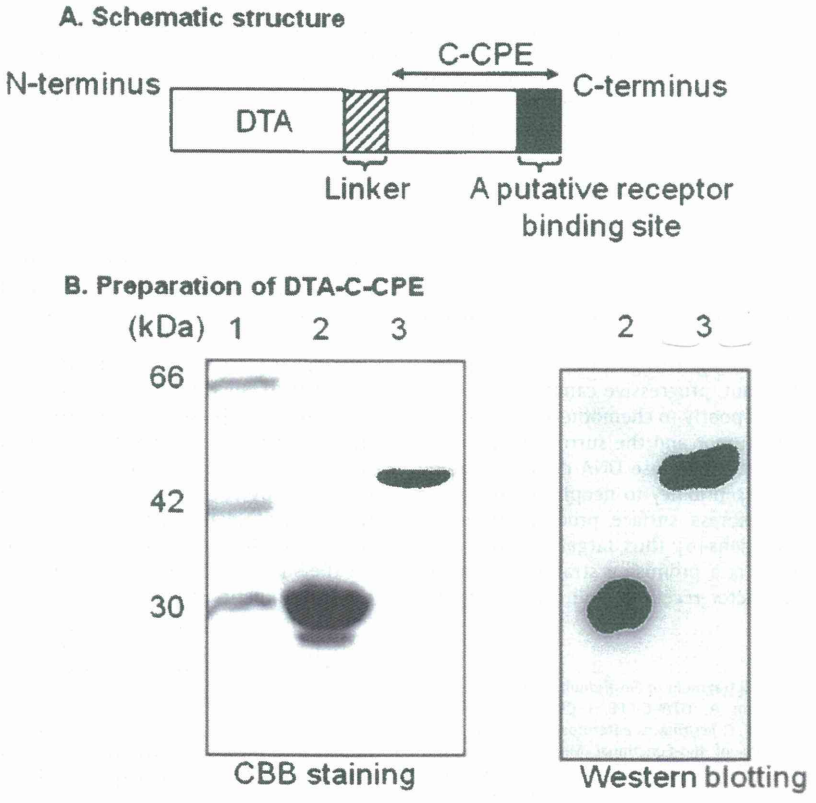

Fig. 1. Preparation of DTA–C-CPE. (A) Schematic structure of DTA–C-CPE. DTA–C-CPE is a fusion protein of DTA and C-CPE with a linker indicated by a slashed column. A dark column indicates a putative receptor-binding region of C-CPE. (B) Preparation of DTA–C-CPE. DTA or DTA–C-CPE was produced by a conventional expression system of *E. coli*, and the proteins were purified by His-tag affinity chromatography with Ni-resins. The purification of DTA–C-CPE was confirmed by SDS–PAGE followed by staining with Coomassie Brilliant Blue (CBB) (left panel in B) and by Western blotting using an anti-His-tag mAb (right panel in B). Lane 1, a marker of molecular size; lane 2, DTA; lane 3, DTA–C-CPE. The putative molecular sizes of DTA and DTA–C-CPE were 30 and 43.2 kDa, respectively.

The plasmid, pET–DTA-linker-C-CPE, was transduced into *Escherichia coli* strain BL21 (DE3), after which the cells were cultured in LB medium supplemented with 100 μg/ml ampicillin at 37 °C until the logarithmic phase. Isopropyl-D-thiogalactopyranoside (0.25 mM) was added to the medium, and the cells were cultured for an additional 3 h. The cells were harvested and then lysed in buffer A (10 mM Tris–HCl, pH 8.0, 400 mM NaCl, 5 mM $MgCl_2$, 0.1 mM phenylmethylsulfonyl fluoride, 1 mM 2-mercaptoethanol, and 10% glycerol). The lysates were centrifuged, and the resultant supernatant was applied to HiTrap Chelating HP (GE Healthcare, Little Chalfont, UK). DTA–C-CPE was eluted by buffer A containing imidazole. The solvent was exchanged with phosphate-buffered saline by using a PD-10 column (GE Healthcare), and the purified protein was stored at −80 °C until use. Purification of DTA–C-CPE was confirmed by sodium dodecylsulfate polyacrylamide gel electrophoresis, followed by staining with Coomassie Brilliant Blue and immunoblotting with anti-His-tag antibody. Protein was quantified by using a protein assay kit (Pierce Chemical, Rockford, IL) with BSA as a standard.

2.4. Cytotoxic activity

Cell viability was determined by using a tetrazolium-based colorimetric assay or lactate dehydrogenase (LDH) assay. Briefly, cells were seeded into a 96-well plate at 1×10^4 cells per well. On the following day, the cells were treated with DTA or DTA–C-CPE (0–20 μg/ml) for 48 h. In the colorimetric assay, WST-8 was added to the wells, mixed thoroughly and incubated for 1 h. Then, the absorbance was measured at 450 nm. In the LDH assay, the release of LDH from the cells was analyzed by using a CytoTox96 NonRadioactive Cytotoxicity Assay kit (Promega, Madison, WI), according to the manufacturer's protocol. The LDH release was calculated by using the following equation: percentage of maximal LDH release = LDH in the culture medium/total LDH in the culture dish.

2.5. Competition assay

Cells (1×10^4 cells) were pretreated with 0–40 μg/ml C-CPE or BSA for 2 h, and then 1 μg/ml of DTA–C-CPE was added. After an additional 48 h of culture, a colorimetric assay was performed as described previously.

3. Results

3.1. Preparation of DTA–C-CPE

When DTA enters the cytosol, it inhibits elongation factor 2 through ADP-ribosylation and induces the inhibition of protein synthesis, leading to cell death [20,22]. C-CPE is a receptor-binding domain of CPE, and the CL-4-binding region is located on the C-terminal of C-CPE [23]. To prepare a CL-4-targeting molecule, we genetically fused DTA with C-CPE at the N-terminal of C-CPE and C-terminal of DTA. A schematic illustration of DTA–C-CPE is shown in Fig. 1A. DTA–C-CPE was produced in *E. coli* and was purified by affinity chromatography with Ni-resins. The molecular size of DTA–C-CPE, as determined by SDS–PAGE and immunoblotting, was identical to its putative size (43.2 kDa, Fig. 1B).

3.2. Cytotoxic properties of DTA–C-CPE

To examine the cytotoxicity of DTA–C-CPE, we investigated the effects of DTA–C-CPE on CL-4-expressing L (CL4/L) cells. DTA had no effect on CL4/L cells at 20 μg/ml, whereas DTA–C-CPE dose-dependently decreased the viability, reaching 39.7% relative viability at 1 μg/ml (Fig. 2A). Similar results were observed in the LDH-release assay. As shown in Fig. 2B, 5 μg/ml of DTA did not cause a release of cellular LDH; but, DTA–C-CPE at 5 μg/ml significantly increased the release of cellular LDH from 4.7% to 25.0%.

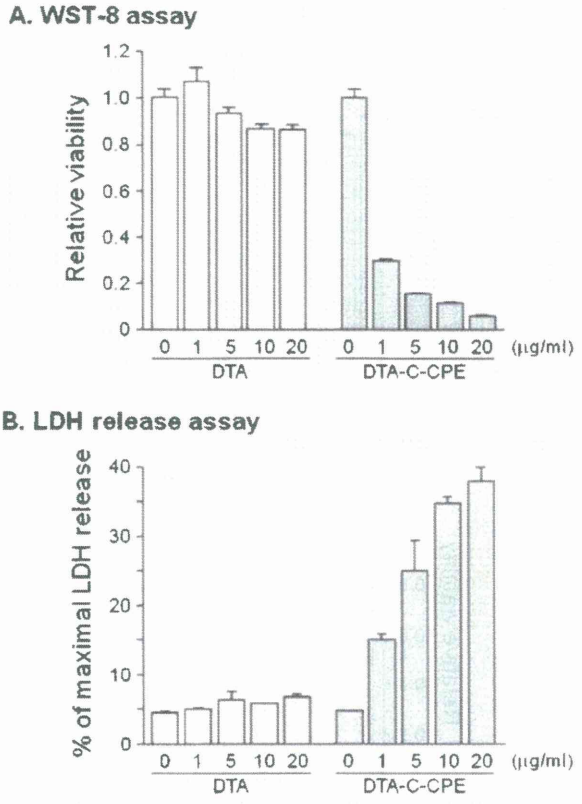

Fig. 2. Cytotoxicity of DTA–C-CPE. CL4/L cells were treated with DTA or DTA–C-CPE at the indicated concentration for 48 h. The cellular viability was measured by WST-8 assay (A) or LDH-release assay (B). Data are the mean ± SD ($n = 3$). The data are representative of three independent experiments.

3.3. Targeting properties of DTA–C-CPE

To confirm the CL specificity of DTA–C-CPE, we evaluated the cytotoxicity of DTA–C-CPE in L cells that expressed CL-1, -2, -4 or -5. DAT-C-CPE did not show severe cytotoxicity in L, CL1/L, CL2/L and CL5/L cells, even at 5 μg/ml, whereas DTA–C-CPE reduced the viability of CL4/L cells to 35.0% and 23.3% of the vehicle-treated cells at 1 and 5 μg/ml, respectively (Fig. 3A). To determine whether DTA–C-CPE bond to CL4/L cells via its C-CPE domain, we performed a competition assay. As shown in Fig. 3B, pretreatment of the cells with C-CPE dose-dependently attenuated the cytotoxic activity of DTA–C-CPE from 41.3% to 90.9% of viability at 0–40 μg/ml of C-CPE. In contrast, pretreatment of the cells with BSA at 40 μg/ml did not affect the cytotoxicity of DTA–C-CPE, indicating that DTA–C-CPE bound to the cells via its C-CPE domain. Thus, fusion of C-CPE gives a CL-4-targeting property to DTA, producing a CL-4-specific cytotoxic agent.

4. Discussion

CL-4 is often overexpressed in some malignant tumors, such as breast, prostate, ovarian, pancreatic and gastric cancers [12,14,17]. CL-4 targeting is a promising method for tumor-targeting therapy. In the present study, we prepared a fusion protein of DTA, a protein

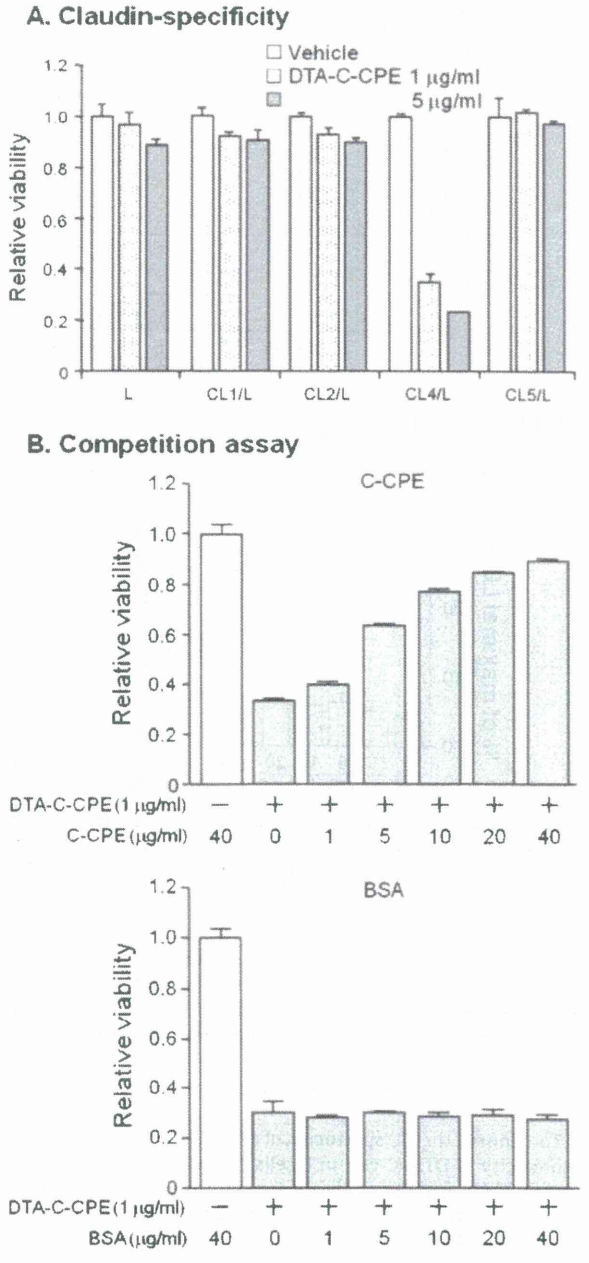

Fig. 3. Cytotoxic properties of DTA–C-CPE. (A) Claudin-specificity. L, CL1/L, CL2/L, CL4/L or CL5/L cells were treated with DTA–C-CPE at the indicated concentration for 48 h. After incubation, the cellular viability was measured by WST-8 assay. Data are the mean ± SD ($n = 3$). The data are representative of three independent experiments. (B) Competition assay. CL-4/L cells were pretreated with C-CPE (upper panel) or BSA (lower panel) at the indicated concentration for 2 h, and then the cells were treated with DAT-C-CPE (1 μg/ml) for 48 h. The cellular viability was measured by WST-8 assay. Data are the mean ± SD ($n = 3$). The data are representative of three independent experiments.

synthesis inhibitory factor, and C-CPE, which binds to CL-4, and we found that the fused protein (DTA–C-CPE) is toxic to CL-4-expressing cells.

DTA kills cells by inactivating elongation factor 2 when one molecule of this protein is introduced into the cytosol [24]. DTA permits the successful targeting of cells displaying only a limited number of tumor-specific growth factor receptors or antigens overexpressed on their surface, and immunotoxins containing DTA, ONTAK and DT 388GMCSF are used clinically for cancer-targeted therapy [25–27]. Therefore, we selected DTA as a cytotoxic molecule for the present study.

A CL-4-targeting molecule containing DTA needs to bind to CL-4 and enter the cytosol. C-CPE is the receptor-binding domain of CPE, and the CL-4-binding region is located on the C-terminal of C-CPE [15,23,28]. CL-4 has a sorting signal to clathrin-coated vehicles, and CL-4 is expected to be taken up by clathrin-mediated endocytosis [29–31]. CL-4 bound to DTA–C-CPE may be taken up by the endocytotic pathway, followed by release of DTA from endosomes into the cytosol. Further studies are needed to elucidate the detailed mechanism of DTA–C-CPE-induced cell death.

Reduced side effects and increased anti-tumor effects are pivotal characteristics needed for anti-tumor agents. Targeting cancer cells by using ligands for growth factor receptors or antigens that are overexpressed on the cell membrane is a potent strategy, and the success of the targeted therapy depends on the target molecule selection. The CL family has attractive characteristics for their use as targets in tumor therapy. First, CL has two extracellular loop domains that can be target sites [12]. Second, CLs are overexpressed in nine of 12 cancer types, creating a differential expression profile between tumor cells and normal cells [12,14]. Third, CLs are often exposed on the apical membrane in cancer cells, whereas CLs are located in the intercellular junction between adjacent cells in normal cells [14]. Even if the CL level in tumors is not more than the level in normal tissues, CL may be more accessible in the tumor. Thus, CLs have great promise as targets for tumor therapy. C-CPE is a CL ligand. We prepared C-CPE-PSIF, a lead compound for tumor therapy, by using the CL-4-targeting ligand C-CPE [32]. We already determined the functional domains of C-CPE as a CL-4-targeting molecule, and we are using C-CPE as a prototype to develop a novel CL ligand. This is the first study to produce CL-4-targeted DTA. Future development of the CL-4-targeting immunotoxin using DTA and a CL ligand will provide a novel tumor-targeted therapy.

Acknowledgements

We thank Dr. Y. Horiguchi (Osaka University) and the members of our laboratory for providing us C-CPE cDNA and their useful comments and discussion, respectively. This work was supported by a Grant-in-Aid for Scientific Research from the Ministry of Education, Culture, Sports, Science and Technology, Japan (21689006) and by Health and Labor Sciences Research Grants from the Ministry of Health, Labor, and Welfare of Japan.

References

[1] S. Marchini, M. D'Incalci, M. Broggini, New molecules and strategies in the field of anticancer agents, Curr. Med. Chem. Anticancer Agents 4 (2004) 247–262.
[2] D.A. Rew, G.D. Wilson, Cell production rates in human tissues and tumours and their significance. Part 1: an introduction to the techniques of measurement and their limitations, Eur. J. Surg. Oncol. 26 (2000) 227–238.
[3] S. Potala, S.K. Sahoo, R.S. Verma, Targeted therapy of cancer using *diphtheria* toxin-derived immunotoxins, Drug Discov. Today 13 (2008) 807–815.
[4] W.F. Benedict, M.S. Baker, L. Haroun, E. Choi, B.N. Ames, Mutagenicity of cancer chemotherapeutic agents in the Salmonella/microsome test, Cancer Res. 37 (1977) 2209–2213.
[5] W. Zumkeller, P.N. Schofield, Growth factors, cytokines and soluble forms of receptor molecules in cancer patients, Anticancer Res. 15 (1995) 343–348.
[6] R.J. Kreitman, I. Pastan, Immunotoxins in the treatment of hematologic malignancies, Curr. Drug Targets 7 (2006) 1301–1311.
[7] D.W. Powell, Barrier function of epithelia, Am. J. Physiol. 241 (1981) G275–G288.
[8] J.M. Mullin, Potential interplay between luminal growth factors and increased tight junction permeability in epithelial carcinogenesis, J. Exp. Zool. 279 (1997) 484–489.
[9] A. Martinez-Palomo, Ultrastructural modifications of intercellular junctions between tumor cells, In Vitro 6 (1970) 15–20.
[10] J.G. Swift, T.M. Mukherjee, R. Rowland, Intercellular junctions in hepatocellular carcinoma, J. Submicrosc. Cytol. 15 (1983) 799–810.

[11] P.D. Vermeer, L.A. Einwalter, T.O. Moninger, T. Rokhlina, J.A. Kern, J. Zabner, M.J. Welsh, Segregation of receptor and ligand regulates activation of epithelial growth factor receptor, Nature 422 (2003) 322–326.
[12] P.J. Morin, Claudin proteins in human cancer: promising new targets for diagnosis and therapy, Cancer Res. 65 (2005) 9603–9606.
[13] M. Furuse, S. Tsukita, Claudins in occluding junctions of humans and flies, Trends Cell Biol. 16 (2006) 181–188.
[14] S.L. Kominsky, Claudins: emerging targets for cancer therapy, Expert Rev. Mol. Med. 8 (2006) 1–11.
[15] J. Katahira, N. Inoue, Y. Horiguchi, M. Matsuda, N. Sugimoto, Molecular cloning and functional characterization of the receptor for *Clostridium perfringens* enterotoxin, J. Cell Biol. 136 (1997) 1239–1247.
[16] S.L. Kominsky, M. Vali, D. Korz, T.G. Gabig, S.A. Weitzman, P. Argani, S. Sukumar, *Clostridium perfringens* enterotoxin elicits rapid and specific cytolysis of breast carcinoma cells mediated through tight junction proteins claudin 3 and 4, Am. J. Pathol. 164 (2004) 1627–1633.
[17] A.D. Santin, S. Cane, S. Bellone, M. Palmieri, E.R. Siegel, M. Thomas, J.J. Roman, A. Burnett, M.J. Cannon, S. Pecorelli, Treatment of chemotherapy-resistant human ovarian cancer xenografts in C.B-17/SCID mice by intraperitoneal administration of *Clostridium perfringens* enterotoxin, Cancer Res. 65 (2005) 4334–4342.
[18] P. Michl, M. Buchholz, M. Rolke, S. Kunsch, M. Lohr, B. McClane, S. Tsukita, G. Leder, G. Adler, T.M. Gress, Claudin-4: a new target for pancreatic cancer treatment using *Clostridium perfringens* enterotoxin, Gastroenterology 121 (2001) 678–684.
[19] N. Sonoda, M. Furuse, H. Sasaki, S. Yonemura, J. Katahira, Y. Horiguchi, S. Tsukita, *Clostridium perfringens* enterotoxin fragment removes specific claudins from tight junction strands: Evidence for direct involvement of claudins in tight junction barrier, J. Cell Biol. 147 (1999) 195–204.
[20] R.J. Collier, *Diphtheria* toxin: mode of action and structure, Bacteriol. Rev. 39 (1975) 54–85.
[21] D. Leong, K.D. Coleman, J.R. Murphy, Cloned fragment A of *diphtheria* toxin is expressed and secreted into the periplasmic space of *Escherichia coli* K12, Science 220 (1983) 515–517.
[22] P.O. Falnes, K. Sandvig, Penetration of protein toxins into cells, Curr. Opin. Cell Biol. 12 (2000) 407–413.
[23] P.C. Hanna, T.A. Mietzner, G.K. Schoolnik, B.A. McClane, Localization of the receptor-binding region of *Clostridium perfringens* enterotoxin utilizing cloned toxin fragments and synthetic peptides. The 30 C-terminal amino acids define a functional binding region, J. Biol. Chem. 266 (1991) 11037–11043.
[24] M. Yamaizumi, E. Mekada, T. Uchida, Y. Okada, One molecule of *diphtheria* toxin fragment A introduced into a cell can kill the cell, Cell 15 (1978) 245–250.
[25] F. Foss, Clinical experience with denileukin diftitox (ONTAK), Semin. Oncol. 33 (2006) S11–S16.
[26] A.E. Frankel, D.R. Fleming, P.D. Hall, B.L. Powell, J.H. Black, C. Leftwich, R. Gartenhaus, A phase II study of DT fusion protein denileukin diftitox in patients with fludarabine-refractory chronic lymphocytic leukemia, Clin. Cancer Res. 9 (2003) 3555–3561.
[27] A.E. Frankel, B.L. Powell, P.D. Hall, L.D. Case, R.J. Kreitman, Phase I trial of a novel *diphtheria* toxin/granulocyte macrophage colony-stimulating factor fusion protein (DT 388GMCSF) for refractory or relapsed acute myeloid leukemia, Clin. Cancer Res. 8 (2002) 1004–1013.
[28] A. Takahashi, M. Kondoh, A. Masuyama, M. Fujii, H. Mizuguchi, Y. Horiguchi, Y. Watanabe, Role of C-terminal regions of the C-terminal fragment of *Clostridium perfringens* enterotoxin in its interaction with claudin-4, J. Control. Release 108 (2005) 56–62.
[29] J.S. Bonifacino, L.M. Traub, Signals for sorting of transmembrane proteins to endosomes and lysosomes, Annu. Rev. Biochem. 72 (2003) 395–447.
[30] A.I. Ivanov, A. Nusrat, C.A. Parkos, Endocytosis of epithelial apical junctional proteins by a clathrin-mediated pathway into a unique storage compartment, Mol. Biol. Cell 15 (2004) 176–188.
[31] M. Matsuda, A. Kubo, M. Furuse, S. Tsukita, A peculiar internalization of claudins, tight junction-specific adhesion molecules, during the intercellular movement of epithelial cells, J. Cell Sci. 117 (2004) 1247–1257.
[32] C. Ebihara, M. Kondoh, N. Hasuike, M. Harada, H. Mizuguchi, Y. Horiguchi, M. Fujii, Y. Watanabe, Preparation of a claudin-targeting molecule using a C-terminal fragment of *Clostridium perfringens* enterotoxin, J. Pharmacol. Exp. Ther. 316 (2006) 255–260.

National Institute of Biomedical Innovation (NiBio)[1]; Graduate School of Pharmaceutical Sciences[2], Osaka University; The Center for Advanced Medical Engineering and Informatics[3], Osaka University, Osaka, Japan

Creation of an improved mutant TNF with TNFR1-selectivity and antagonistic activity by phage display technology

T. NOMURA[1,2*], Y. ABE[1*], H. KAMADA[1,3], M. INOUE[1], T. KAWARA[1,2], S. ARITA[1,2], T. FURUYA[1,2], K. MINOWA[1], Y. YOSHIOKA[2,3], H. SHIBATA[1], H. KAYAMURO[1,2], T. YAMASHITA[1,2], K. NAGANO[1], T. YOSHIKAWA[1,2], Y. MUKAI[2], S. NAKAGAWA[2,3], S. TSUNODA[1,2,3], Y. TSUTSUMI[1,2,3]

Received August 7, 2009, accepted August 14, 2009

Shin-ichi Tsunoda, Ph.D., Laboratory of Pharmaceutical Proteomics, National Institute of Biomedical Innovation, 7-6-8 Saito-Asagi, Ibaraki, Osaka 567-0085, Japan
tsunoda@nibio.go.jp
**These authors contributed equally to the work.*

Pharmazie 65: 93–96 (2010) *doi: 10.1691/ph.2010.9265*

Tumor necrosis factor-α (TNF), which binds two types of TNF receptors (TNFR1 and TNFR2), regulates the onset and exacerbation of autoimmune diseases such as rheumatoid arthritis and Crohn's disease. In particular, TNFR1-mediated signals are predominantly related to the induction of inflammatory responses. We have previously generated a TNFR1-selective antagonistic TNF-mutant (mutTNF) and shown that mutTNF efficiently inhibits TNFR1-mediated bioactivity *in vitro* and attenuates inflammatory conditions *in vivo*. In this study, we aimed to improve the TNFR1-selectivity of mutTNF. This was achieved by constructing a phage library displaying mutTNF-based variants, in which the amino acid residues at the predicted receptor binding sites were substituted to other amino acids. From this mutant TNF library, 20 candidate TNFR1-selective antagonists were isolated. Like mutTNF, all 20 candidates were found to have an inhibitory effect on TNFR1-mediated bioactivity. However, one of the mutants, N7, displayed significantly more than 40-fold greater TNFR1-selectivty than mutTNF. Therefore, N7 could be a promising anti-autoimmune agent that does not interfere with TNFR2-mediated signaling pathways.

1. Introduction

The severity and progression of inflammatory diseases, such as rheumatoid arthritis, Crohn's disease and ulcerative colitis, can be correlated with the serum level of tumor necrosis factor-α (TNF). Thus, TNF blockades such as anti-TNF antibodies and soluble TNFRs, which neutralize the activity of TNF, have been used to treat various autoimmune diseases in clinical practice. However, TNF blockades inhibit both TNFR1 and TNFR2 signaling. Thus, treatment with these drugs can lead to an increased risk of infection (Gomez-Reino et al. 2003; Lubel et al. 2007) and lymphoma development (Brown et al. 2002). TNF has been reported to induce inflammatory response predominantly through TNFR1 (Mori et al. 1996), whereas activation of the immune response is initiated *via* TNFR2 (Kim et al. 2006; Kim and Teh 2001; Grell et al. 1998). Therefore, blocking TNFR1-signaling, but not TNFR2-signaling, is a promising strategy for the safe and effective treatment of inflammatory diseases, which overcomes the risk of infection associated with the use of non-specific TNF blockades (Kollias and Kontoyiannis 2002).
In our previous studies, we used the phage display technique (Imai et al. 2008; Nagano et al. 2009; Nomura et al. 2007) to generate a TNFR1-selective antagonistic mutant TNF (mutTNF) that blocks TNFR1-mediated signals but not those of TNFR2 (Shibata et al. 2008b). Moreover, mutTNF showed superior therapeutic effects using an inflammatory disease mouse model (Shibata et al. 2008a). Thus, a drug for autoimmune diseases that selectively targets TNFR1 is anticipated to display higher efficacy and safety compared to existing treatments. In this study, we have attempted to isolate TNFR1-selective antagonists with higher TNFR1-selectivity than previous mutTNF by constructing a modified phage library displaying mutTNF-based variants.

2. Investigations, results and discussion

Here, we attempted to improve the TNFR1-selectivity of mutTNF using a phage display technique. Firstly, we constructed a phage library of TNF mutant using mutTNF as template. We designed a randomized library of mutTNF to replace the six amino acid residues (aa 29, 31, 32, 145–147) in the predicted receptor binding site. As a result of the 2-step PCR, we confirmed that the mutTNF mutant library consisted of 4×10^7 independent recombinant clones (*data not shown*). To enrich for TNFR1-selective antagonists, the phage library was subjected to two rounds of panning against TNFR1 on a Biacore biosensor chip. After the second panning, supernatants of single clone of *E. coli* TG1 including phagemid were randomly collected and subjected to screening by bioassay and ELISA to evaluate their bioactivity and affinity against each TNF receptor, respectively (*data not shown*). Consequently, twenty candidates of TNFR1-selective mutants with antagonistic activity were isolated (Table).
Next, we determined the detailed biological properties of each candidate. Positive clones were engineered for expression in

Table: Amino acid sequences and biological properties of TNFR1-selective antagonist candidates

TNF	Amino acid sequence						Relative affinity (% K_d)[a]			Bioactivity via TNFR1	
	29	31	32	145	146	147	TNFR1	TNFR2	TNFR1[b]/TNCR2	Agonistic[c] activity	Antagonisti[d] activity
mutTNF	L	R	R	A	E	S	100.0	100.0	1.0	–	+
N1	S	–	W	R	–	–	550.0	21.6	25.5	+	–
N2	S	–	W	–	–	–	200.0	N.D.	N.D.	+	–
N3	S	–	W	R	D	–	550.0	44.8	12.3	–	±
N4	S	–	W	–	D	–	183.3	19.1	9.6	±	–
N5	S	–	W	–	S	E	275.0	25.8	10.7	±	–
N6	A	D	T	–	–	–	200.0	21.6	9.3	±	–
N7	S	N	D	D	A	–	104.7	2.5	41.9	–	+
N8	R	I	A	D	–	–	169.2	26.7	6.3	+	–
N9	H	H	–	–	N	G	169.2	33.0	5.1	+	–
N10	T	N	N	–	–	–	314.3	28.6	11.0	±	–
N11	T	N	N	S	–	–	275.0	18.3	15.0	±	–
N12	F	S	T	–	–	–	440.0	58.0	7.6	+	–
N13	F	S	T	–	S	E	440.0	73.9	6.0	+	–
N14	R	W	Y	T	N	T	314.3	19.2	16.4	+	–
N15	F	K	T	N	A	T	275.0	24.1	11.4	±	–
N16	M	L	T	N	S	T	367.0	7.7	47.7	+	–
N17	Y	L	A	T	H	T	137.5	1.6	86.0	±	–
N18	Y	L	A	T	H	–	110.0	4.7	23.4	±	–
N19	V	Q	Y	N	N	–	367.0	N.D.	N.D.	±	–
N20	F	S	T	P	Q	R	244.4	N.D.	N.D.	±	–

Conserved residues compared with mutTNF are indicated by an em dash (–) The affinity values are shown as relative values (% mutTNF). N.D.: not detected

[a] Affinity for immobilized TNFR1 and TNFR2 was assessed by SPR using BIAcore3000. The dissociation constant (K_d) of TNF mutants were calculated from their sensorgrams by BIAEVALUATION 4.0 software

[b] TNFR1-selectivity was defined as relative affinity [TNFE1]/ relative affinity [TNFR2] for mutTNF

[c] TNFR1-mediated agonistic activity was measured, using a HEp-2 cell cytotoxicity assay. The intensity in agonistic activity was evaluated as the following. Cell viability at 10^4 ng/ml each mutant. 0–25% (of non treatment); (+), 25–50%; (±), 50–100%; (–)

[d] TNFR1-mediated antagonistic activity of mutant TNFs on wtTNF induced cytotoxicity in HEp-2 cells was measured. The intensity in antagonistic activity was evaluated as the following. Cell viability at 10^5 ng/ml each mutant in present of 5 ng/ml wtTNF. 0–25% (of non treatment); (–), 25–50%; (±), 50–100%; (+)

E. coli BL21λDE3 and each recombinant protein was purified as described previously (Yamamoto 2003). As anticipated, gel electrophoresis confirmed the mutant TNF proteins to have a molecular weight of 17 kDa. Moreover, gel filtration chromatography established that each mutant forms a homotrimeric complex in solution, as is the case for wild-type TNF (wtTNF) (*data not shown*). To analyze the binding properties of these TNFR1-selective TNF candidates, their dissociation constants (K_d) for TNFR1 and TNFR2 were measured using a surface plasmon resonance (SPR) analyzer. Our previous SPR analysis showed that although mutTNF has an almost identical affinity to TNFR1 as to wtTNF, it displays more than 17,000-fold greater selectivity for TNFR1. As shown in the Table, all the candidates exhibited higher affinity for TNFR1 than mutTNF. Furthermore, clones N1, N7, N16, N17 and N18 showed more than 20-fold higher TNFR1-binding selectivity compared to mutTNF. To examine the bioactivity of all candidates *via* TNFR1, we subsequently performed a cytotoxicity assay using

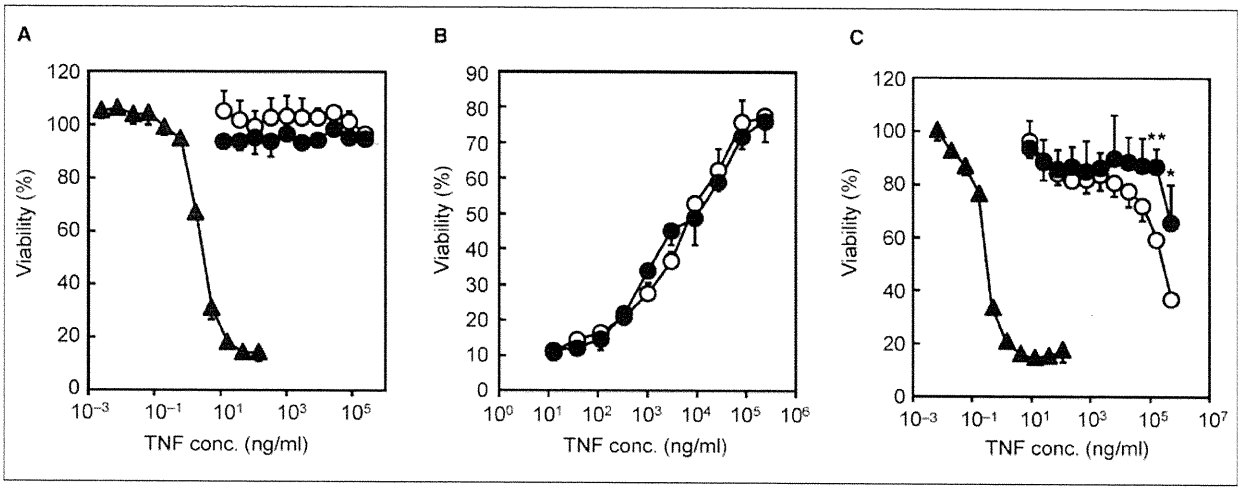

Fig.: Bioactivities and antagonistic activities of N7. (A) To determine the TNFR1-mediated bioactivities, several dilutions of wtTNF (closed triangle), mutTNF (open circle) and N7 (closed circle) were added to L-M cells and incubated for 4 h at 37 °C. (B) Indicated dilutions of mutTNF (open circle) and N7 (closed circle) and constant of wtTNF (5 ng/ml) were mixed and added to L-M cells and incubated for 4 h at 37 °C. TNFR1-mediated antagonistic activity was assessed as described in the Experimental section. (C) To determine the TNFR2-mediated bioactivities, diluted wtTNF (closed triangle), mutTNF (open circle) and N7 (closed circle) were added to hTNFR2/mFas-preadipocyte cells and incubated for 48 h at 37 °C. After incubation, cell viability was measured using the methylene blue assay. Data represent the mean ± S.D. and were analyzed by Student's t-test (*$p < 0{,}05$, **$p < 0{,}01$ vs mutTNF)

HEp-2 cells (Table). As anticipated, mutTNF was unable to activate TNFR1. Likewise clones N3 and N7 do not activate TNFR1 signaling, even when tested at high concentrations. The TNFR1-mediated antagonistic assay demonstrated that N7 showed the highest activity of all the TNFR1-selective antagonist candidates. The Figure show details of bioactivities and antagonistic activities of N7. The TNFR1-mediated agonistic activity using L-M cells showed that wtTNF displays TNFR1-mediated agonistic activity in a dose-dependent manner. In contrast, N7, in addition to mutTNF, barely displays any agonistic activity (Fig. A). Moreover, N7 had an almost identical antagonistic activity for TNFR1-mediated bioactivity to that of mutTNF (Fig. B). Next, TNFR2-mediated activities of these TNFR1-selective antagonists were measured using hTNFR2/mFas-preadipocyte cells. The bioactivity of mutTNF and N7 *via* TNFR2 was much lower than that of wtTNF. Remarkably, TNFR2-mediated agonistic activity of N7 was lower than that of mutTNF, in agreement with the reduced affinity for TNFR2 (Fig. C).

In conclusion, we have succeeded in creating a TNFR1-selective antagonist with improved TNFR1-selectivity over that of mutTNF. This was achieved by constructing a library of mutTNF variants using a phage display technique. While TNFR1 is believed to be important for immunological responses (Rothe et al. 1993), TNFR2 is thought to be important for antiviral resistance and is effective for controlling mycobacterial infection by affecting membrane-bound TNF stimulation (Saunders et al. 2005; Olleros et al. 2002). Therefore, use of N7 might reduce the risk of side effects, such as infections, when applying TNF blockade as a therapy for autoimmune disease. We are currently evaluating the therapeutic effect of N7 using a mouse autoimmune disease model.

3. Experimental

3.1. Cell culture

HEp-2 cells (a human fibroblast cell line) were provided by Cell Resource Center for Biomedical Research (Tohoku University, Sendai) and were maintained in RPMI 1640 medium supplemented with 10% FBS and 1% antibiotics cocktail (penicillin 10,000 units/ml, streptomycin 10 mg/ml, and amphotericin B 25 μg/ml). L-M cells (a mouse fibroblast cell line) were provided by Mochida Pharmaceutical Co. Ltd. (Tokyo, Japan) and were maintained in minimum Eagle's medium supplemented with 1% FBS and 1% antibiotics cocktail. hTNFR2/mFas-preadipocyte cells were established previously in our laboratory (Abe et al. 2008) and were maintained in Dulbecco's modified Eagle's medium supplemented with Blasticidin S HCl, 10% FBS, 1 mM sodium pyruvate, 5×10^{-5} M 2-mercaptoethanol, and 1% antibiotic cocktail.

3.2. Construction of a novel gene library displaying mutTNF variants

The pCANTAB phagemid vector encoding mutTNF was used as template for PCR. The mutTNF was created in previous study and showed TNFR1-selective antagonistic activity (Shibata et al. 2008b). The six amino acid residues at the receptor binding site (amino acid residues; 29, 31, 32 and 145–147) of mutTNF were replaced with other amino acids using a 2-step PCR procedure as described previously (Mukai et al. 2009).

3.3. Selection of TNFR1-selective antagonist candidates from a mutTNF mutated phage library

Human TNFR1 Fc chimera (R&D systems, Minneapolis, MN) was immobilized onto a CM3 sensor chip as described previously. Briefly, the phage display library (1×10^{11} CFU/100 μl) was injected over the sensor chip at a flow rate of 3 μl/min. After binding, the sensor chip was washed using the rinse command until the association phase was reached. Elution was carried out using 4 μl of 10 mM glycine-HCl. The eluted phage pool was neutralized with 1 M Tris-HCl (pH 6.9) and then used to infect *E. coli* TG1 in order to amplify the phage. The panning steps were repeated twice. Subsequently, single clones were isolated and supernatant from each clone was collected and used to determine the cytotoxicity in the HEp-2 cytotoxic assay and the affinity for TNFR1 by ELISA, respectively (Shibata et al. 2008b). We screened clones having almost no cytotoxicity but significant affinity for TNFR1. The phagemids purified from single clones were sequenced using the Big Dye Terminator v3.1 kit (Applied Biosystems, Foster City, CA). Sequencing reactions were analyzed on an ABI PRISM 3100 (Applied Biosystems).

3.4. Surface plasmon resonance assay (BIAcore® assay)

The binding kinetics of the proteins were analyzed by the surface plasmon resonance technique by BIAcore® (GE Healthcare, Amersham, UK). Each TNF receptor was immobilized onto a CM5 sensor chip, which resulted in an increase of 3,000–3,500 resonance units. During the association phase, all clones serially diluted in running buffer (HBS-EP) were allowed to pass over TNFR1 and TNFR2 at a flow rate of 20 μl/min. Kinetic parameters for each candidate were calculated from the respective sensorgram using BIAevaluation 4.0 software.

3.5. Cytotoxicity assay

In order to measure TNFR1-mediated cytotoxicity, HEp-2 or L-M cells were cultured in 96-well plates in the presence of TNF mutants and serially diluted wtTNF (Peprotech, Rocky Hill, NJ) with 100 μg/ml cycloheximide for 18 h at 4×10^4 cells/well or for 48 h at 1×104 cells/well. Cytotoxicity was then assessed using the methylene blue assay as described previously (Mukai et al. 2009; Shibata et al. 2004). For the TNFR1-mediated antagonistic assay, cells were cultured in the presence of 5 ng/ml human wtTNF and a serial dilution of the mutTNF. For the TNFR2-mediated cytotoxic assay, hTNFR2/mFas-preadipocyte cells were cultured in 96-well plates in the presence of TNF mutants and serially diluted wtTNF (1×10^4 cells/well) (Abe et al. 2008). After incubation for 48 h, cell survival was determined using the methylene blue assay.

Acknowledgement: This study was supported in part by Grants-in-Aid for Scientific Research from the Ministry of Education, Culture, Sports, Science and Technology of Japan, and by Grants-in-Aid for Scientific Research from Japan Society for the Promotion of Science (JSPS). In addition, this study was also supported in part by Health Labour Sciences Research Grants from the Ministry of Health, Labor and Welfare of Japan, Health Sciences Research Grants for Research on Publicly Essential Drugs and Medical Devices from the Japan Health Sciences Foundation and by a Grant from the Minister of the Environment, as well as THE NAGAI FOUNDATION TOKYO.

References

Abe Y, Yoshikawa T, Kamada H, Shibata H, Nomura T, Minowa K, Kayamuro H, Katayama K, Miyoshi H, Mukai Y, Yoshioka Y, Nakagawa S, Tsunoda S, Tsutsumi Y (2008) Simple and highly sensitive assay system for TNFR2-mediated soluble- and transmembrane-TNF activity. J Immunol Methods 335: 71–78.

Aggarwal BB (2003) Signalling pathways of the TNF superfamily: a double-edged sword. Nat Rev Immunol 3: 745–756.

Brown SL, Greene MH, Gershon SK, Edwards ET, Braun MM (2002) Tumor necrosis factor antagonist therapy and lymphoma development: twenty-six cases reported to the Food and Drug Administration. Arthritis Rheum 46: 3151–3158.

Feldmann M (2002) Development of anti-TNF therapy for rheumatoid arthritis. Nat Rev Immunol 2: 364–371.

Goldbach-Mansky R, Lipsky PE (2003) New concepts in the treatment of rheumatoid arthritis. Annu Rev Med 54: 197–216.

Gomez-Reino JJ, Carmona L, Valverde VR, Mola EM, Montero MD (2003) Treatment of rheumatoid arthritis with tumor necrosis factor inhibitors may predispose to significant increase in tuberculosis risk: a multicenter active-surveillance report. Arthritis Rheum 48: 2122–2127.

Grell M, Becke FM, Wajant H, Mannel DN, Scheurich P (1998) TNF receptor type 2 mediates thymocyte proliferation independently of TNF receptor type 1. Eur J Immunol 28: 257–263.

Imai S, Mukai Y, Takeda T, Abe Y, Nagano K, Kamada H, Nakagawa S, Tsunoda S, Tsutsumi Y (2008) Effect of protein properties on display efficiency using the M13 phage display system. Pharmazie 63: 760–764.

Kim EY, Priatel JJ, Teh SJ, Teh HS (2006) TNF receptor type 2 (p75) functions as a costimulator for antigen-driven T cell responses *in vivo*. J Immunol 176: 1026–1035.

Kim EY, Teh HS (2001) TNF type 2 receptor (p75) lowers the threshold of T cell activation. J Immunol 167: 6812–6820.

Kollias G, Kontoyiannis D (2002) Role of TNF/TNFR in autoimmunity: specific TNF receptor blockade may be advantageous to anti-TNF treatments. Cytokine Growth Factor Rev 13: 315–321.

Lubel JS, Testro AG, Angus PW (2007) Hepatitis B virus reactivation following immunosuppressive therapy: guidelines for prevention and management. Intern Med J 37: 705–712.

Mori L, Iselin S, De Libero G, Lesslauer W (1996) Attenuation of collagen-induced arthritis in 55-kDa TNF receptor type 1 (TNFR1)-IgG1-treated and TNFR1-deficient mice. J Immunol 157: 3178–3182.

Mukai Y, Shibata H, Nakamura T, Yoshioka Y, Abe Y, Nomura T, Taniai M, Ohta T, Ikemizu S, Nakagawa S, Tsunoda S, Kamada H, Yamagata Y, Tsutsumi Y (2009) Structure-function relationship of tumor necrosis factor (TNF) and its receptor interaction based on 3D structural analysis of a fully active TNFR1-selective TNF mutant. J Mol Biol 385: 1221–1229.

Nagano K, Imai S, Mukai Y, Nakagawa S, Abe Y, Kamada H, Tsunoda S, Tsutsumi Y (2009) Rapid isolation of intrabody candidates by using an optimized non-immune phage antibody library. Pharmazie 64: 238–241.

Nomura T, Kawamura M, Shibata H, Abe Y, Ohkawa A, Mukai Y, Sugita T, Imai S, Nagano K, Okamoto T, Tsutsumi Y, Kamada H, Nakagawa S, Tsunoda S (2007) Creation of a novel cell penetrating peptide, using a random 18mer peptides library. Pharmazie 62: 569–573.

Olleros ML, Guler R, Corazza N, Vesin D, Eugster HP, Marchal G, Chavarot P, Mueller C, Garcia I (2002) Transmembrane TNF induces an efficient cell-mediated immunity and resistance to Mycobacterium bovis bacillus Calmette-Guerin infection in the absence of secreted TNF and lymphotoxin-alpha. J Immunol 168: 3394–3401.

Rothe J, Lesslauer W, Lotscher H, Lang Y, Koebel P, Kontgen F, Althage A, Zinkernagel R, Steinmetz M, Bluethmann H (1993) Mice lacking the tumour necrosis factor receptor 1 are resistant to TNF-mediated toxicity but highly susceptible to infection by Listeria monocytogenes. Nature 364: 798–802.

Saunders BM, Tran S, Ruuls S, Sedgwick JD, Briscoe H, Britton WJ (2005) Transmembrane TNF is sufficient to initiate cell migration and granuloma formation and provide acute, but not long-term, control of Mycobacterium tuberculosis infection. J Immunol 174: 4852–4859.

Shibata H, Yoshioka Y, Ikemizu S, Kobayashi K, Yamamoto Y, Mukai Y, Okamoto T, Taniai M, Kawamura M, Abe Y, Nakagawa S, Hayakawa T, Nagata S, Yamagata Y, Mayumi T, Kamada H, Tsutsumi Y (2004) Functionalization of tumor necrosis factor-alpha using phage display technique and PEGylation improves its antitumor therapeutic window. Clin Cancer Res 10: 8293–8300.

Shibata H, Yoshioka Y, Ohkawa A, Abe Y, Nomura T, Mukai Y, Nakagawa S, Taniai M, Ohta T, Mayumi T, Kamada H, Tsunoda S, Tsutsumi Y (2008a) The therapeutic effect of TNFR1-selective antagonistic mutant TNF-alpha in murine hepatitis models. Cytokine 44: 229–233.

Shibata H, Yoshioka Y, Ohkawa A, Minowa K, Mukai Y, Abe Y, Taniai M, Nomura T, Kayamuro H, Nabeshi H, Sugita T, Imai S, Nagano K, Yoshikawa T, Fujita T, Nakagawa S, Yamamoto A, Ohta T, Hayakawa T, Mayumi T, Vandenabeele P, Aggarwal BB, Nakamura T, Yamagata Y, Tsunoda S, Kamada H, Tsutsumi Y (2008b) Creation and X-ray structure analysis of the tumor necrosis factor receptor-1-selective mutant of a tumor necrosis factor-alpha antagonist. J Biol Chem 283: 998–1007.

Yamamoto Y, Tsutsumi Y, Yoshioka Y, Nishibata T, Kobayashi K, Okamoto T, Mukai Y, Shimizu T, Nakagawa S, Nagata S, Mayumi T (2003) Site-specific PEGylation of a lysine-deficient TNF-alpha with full bioactivity. Nat Biotechnol 21: 546–552.

Cytokine 50 (2010) 75–83

Contents lists available at ScienceDirect

Cytokine

journal homepage: www.elsevier.com/locate/issn/10434666

Generation of mouse macrophages expressing membrane-bound TNF variants with selectivity for TNFR1 or TNFR2

Hiroko Shibata [a,b,1], Yasuhiro Abe [a,1], Yasuo Yoshioka [a,c,1], Tetsuya Nomura [a,d], Masaki Sato [a], Hiroyuki Kayamuro [a,d], Tomoyuki Kawara [a,d], Shuhei Arita [a,d], Tsuyoshi Furuya [a,d], Kazuya Nagano [a], Tomoaki Yoshikawa [a,d], Haruhiko Kamada [a,c], Shin-ichi Tsunoda [a,c,d,*], Yasuo Tsutsumi [a,c,d]

[a] National Institute of Biomedical Innovation (NiBio), 7-6-8 Saito-Asagi, Ibaraki, Osaka 567-0085, Japan
[b] National Institute of Health Science (NIHS), Kamiyoga 1-18-1, Setagaya-ku, Tokyo 158-8501, Japan
[c] The Center for Advanced Medical Engineering and Informatics, Osaka University, 1-6 Yamadaoka, Suita, Osaka 565-0871, Japan
[d] Graduate School of Pharmaceutical Sciences, Osaka University, 1-6 Yamadaoka, Suita, Osaka 565-0871, Japan

ARTICLE INFO

Article history:
Received 31 July 2009
Received in revised form 6 November 2009
Accepted 24 November 2009

Keywords:
Transmembrane TNF
TNFR1
TNFR2
Mutant TNF
Lentiviral vector

ABSTRACT

Tumor necrosis factor-alpha (TNF) is expressed on the cell surface as a transmembrane form (tmTNF), that can be released as a soluble form (solTNF) via proteolytic cleavage. These two types of TNF exert their biological functions by binding to one of two TNF receptors, TNFR1 or TNFR2. However, the biological function of tmTNF through these two receptors remains to be determined. Here, we generated macrophages that expressed tmTNF mutants with selectivity for either TNFR1 or TNRF2 as a tool to evaluate signaling through these receptors. Wild-type TNF (wtTNF), TNFR1-selective mutant TNF (mutTNF-R1) or TNFR2-selective mutant TNF (mutTNF-R2) were individually expressed on the TNFR1$^{-/-}$R2$^{-/-}$ mouse macrophages (Mφ) as the tmTNF forms. tm-mutTNF-R1-expressing Mφ exhibited significant selectivity for binding to TNFR1, whereas tm-mutTNF-R2-expressing Mφ only showed a slight selectivity for binding to TNFR2. Signaling by tm-mutTNF-R1-expressing Mφ through the hTNFR2 was weaker than that of tm-wtTNF-expressing Mφ, suggesting that the binding selectivity correlated with functional selectivity. Interestingly, signaling by tm-mutTNF-R2-expressing Mφ through TNFR2 was much stronger than signaling by tm-wtTNF-expressing Mφ, whereas signaling by the corresponding soluble form was weaker than that mediated by wtTNF. These results indicate tmTNF variants might prove useful for the functional analysis of signaling through TNF receptors.

1. Introduction

Tumor necrosis factor alpha (TNF) plays a crucial role in the host defense system [1]. Increased secretion of TNF is involved in the development of autoimmune diseases, such as rheumatoid arthritis (RA) and Crohn's disease [2,3]. Indeed, anti-human TNF antibody and soluble TNF receptor (TNFR), which interfere with the activity of TNF, have been used to treat these diseases, and are expected to be revolutionary therapies due to their excellent therapeutic effects [4]. TNF is primarily produced as a type II transmembrane form (tmTNF) arranged in stable homotrimers [5,6]. A mature, soluble homotrimeric 17-kDa TNF (solTNF) is released from this 26 kDa memTNF *via* proteolytic cleavage by the metalloprotease, TNF converting enzyme (TACE) [7]. Both solTNF and tmTNF induce cell signaling. tmTNF acts through cell–cell contacts to promote juxtacrine signaling, and solTNF acts in a paracrine fashion. The relative contribution of tmTNF and solTNF to overall TNF activity is difficult to elucidate due to the absence of physiologically relevant models. However, evidence for distinct roles for tmTNF and solTNF *in vivo* have been obtained in genetically modified mice. Study of tmTNF knock-in mice revealed that solTNF is required for the development of acute and chronic inflammation, whereas tmTNF supports many processes underlying the development of lymphoid tissue [8]. Mueller et al. also reported that tmTNF has a strong effect upon the course of cellular immune responses *in vivo* and exerts quantitatively and qualitatively distinct functions from solTNF *in vitro* and *in vivo* [9]. Additionally, juxtacrine signaling by tmTNF was shown to be essential for the resolution of inflammation and the maintenance of immunity to the pathogens, *Listeria monocytogenes* and *Mycobacterium tuberculosis* [10–12]. These different functions mediated by the two forms of TNF may help to explain the opposing activities of TNF, such as

* Corresponding author. Address: National Institute of Biomedical Innovation, Laboratory of Pharmaceutical Proteomics, 7-6-8 Saito-Asagi, Ibaraki, Osaka 567-0085, Japan. Tel.: +81 72 639 7014; fax: +81 72 641 9817.
E-mail address: tsunoda@nibio.go.jp (S.-i. Tsunoda).
[1] These authors contributed equally to this work.

1043-4666/$ - see front matter © 2009 Elsevier Ltd. All rights reserved.
doi:10.1016/j.cyto.2009.11.022

its inflammatory and anti-inflammatory effects. However, the factors underlying the different functions of solTNF and tmTNF and the components of the specific signaling cascades induced by the two forms of TNF remain to be elucidated.

solTNF and tmTNF interact with two receptor subtypes, p55 TNF receptor (TNFR1) and p75 TNF receptor (TNFR2) [13], to exert their biological functions. The interaction of solTNF with TNFR and the downstream signaling and functional outcome of that signaling has been extensively studied [14], because signaling by solTNF *via* TNFR1 or TNFR2 can be analyzed *in vitro* using recombinant wild-type TNF, as well as recombinant TNFR1-, and TNFR2-selective mutant TNF (mutTNF). On the other hand, the analysis of tmTNF/TNFR signaling is still poorly understood. tmTNF-expressing cells have previously been reported following transfection into target cells of a TNF gene containing a deletion of the TNF cleavage site [15]. Nanoparticles decorated with solTNF chemically bound to the surface initiate strong TNFR2 responses, and could mimic the bioactivity of tmTNF [16]. However, there are no receptor-selective forms of tmTNF that could be used to analyze tmTNF/TNFR signaling. Moreover, there are few assay systems that can assess the bioactivity of TNF mediated *via* TNFR2 with high sensitively.

In this context, we have used a novel phage-display based screening system to develop TNFR1 or TNFR2-selective mutTNFs to help clarify the biology of TNF/TNFRs interactions. We have already isolated a TNFR1-selective antagonist [17], and both TNFR1 and TNFR2-selective agonists [18]. Additionally, we established a novel cell line hTNFR2/mFas-preadipocyte, which is a simple and highly sensitive, cell death-based assay system for measuring TNFR2-mediated bioactivity [19]. This assay system can assess both solTNF and tmTNF-mediated bioactivity. In this study, we first expressed the TNFR-selective mutTNFs agonists (mutTNF-R1, mutTNF-R2) in TNFR1$^{-/-}$R2$^{-/-}$ macrophages, and we then investigated the possibility of creating TNFR1- and TNFR2-selective tmTNF.

2. Materials and methods

2.1. Cells

The immortalized TNFR1$^{-/-}$R2$^{-/-}$macrophage cell line (DKO Mφ) established from the bone marrow of a TNFR1$^{-/-}$R2$^{-/-}$ mouse was generously provided by Dr. Aggarwal (The University of Texas M.D. Anderson Cancer Center, Houston TX), and cultured in RPMI-1640 medium supplemented with 10% fetal bovine serum (FBS) and 1% antibiotic cocktail (penicillin 10,000 U/ml, streptomycin 10 mg/ml, and amphotericin B 25 μg/ml; Nacalai Tesque, Kyoto, Japan). Human-TNFR2/mouse-Fas-expressing preadipocytes (hTNFR2/mFas-PA) were maintained in Dulbecco's modified Eagle's medium (DMEM; Sigma–Aldrich, Inc., Tokyo, Japan) with 10% FBS, 1% antibiotic cocktail, and 5 μg/ml blasticidin (Bsd) (Invitrogen Corp., Carlsbad, CA). hTNFR2/mFas-PA cells express a chimeric receptor derived from the extracellular and transmembrane domain of human TNFR2 fused to the intracellular domain of mouse Fas [19]. 293T cells and HeLaP4 cells were cultured in DMEM with 10% FBS and 1% antibiotic cocktail. HEp-2 cells are a human laryngeal squamous cell carcinoma cell line, and were cultured in RPMI-1640 medium supplemented with 10% FBS and 1% antibiotic cocktail.

2.2. Surface plasmon resonance (SPR) assay

The binding kinetics of wtTNF, mutTNF-R1 and mutTNF-R2 were analyzed by the SPR technique using a BIAcore 3000 (BIAcore®, GE Healthcare, Buckinghamshire, UK). Human TNFR1 or human TNFR2 Fc chimeras (R&D systems, Minneapolis, MN) were diluted to 50 μg/ml in 10 mM sodium acetate buffer (pH 4.5). TNFRs were immobilized on a CM5 sensor chip, which resulted in an increase of 3000–3500 resonance units (RU). During the association phase, TNFs diluted in running buffer (HBS-EP) at 156.8, 52.3 or 17.4 nM were individually passed over the immobilized TNFRs at a flow rate of 20 μl/min. During the dissociation phase, HBS-EP buffer was applied to the sensor chip at a flow rate of 20 μl/min. The data were analyzed with BIAEVALUATION 3.0 software (BIAcore®) using a 1:1 binding model.

2.3. Cytotoxicity assays

HEp-2 cells were cultured in 96-well plates (4×10^4 cells/well) in a serial dilution of human TNF (Peprotech, Rocky Hill, NJ) or mutTNFs with 100 μg/ml cycloheximide. After incubation for 18 h, cell survival was determined using the methylene blue assay as described previously [17]. hTNFR2/mFas-PA were seeded onto 96-well plates at a density of 1.5×10^4 cells/well in culture medium. Serial dilutions of human TNF or paraformaldehyde-fixed Mφ cells were prepared in DMEM containing 1 μg/ml cycloheximide, and added to each well. After 48 h, cell viability was measured using the WST-assay kit (Nacalai Tesque) according to the manufacturer's instructions.

2.4. Construction of a self-inactivating (SIN) lentiviral vector

Vectors were constructed using standard cloning procedures. A DNA fragment encoding the precursor signal of human TNF was amplified by polymerase chain reaction (PCR) with the following primer pairs : forward primer-1 (5′-GAT TTC GAT ACG TAC GGA AGC TTC GTC GAC ATT AAT TAA GGA CAC CAT GAG CAC TGA AAG CAT GAT CCG GGA CGT GGA GCT GGC CGA GGA GG-3′) containing a SalI site at the 5′-end, reverse primer-1 (5′-AGA GGC TGA GGA ACA AGC ACC GCC TGG AGC CCT GGG GCC CCC CTG TCT TCT TGG GGA GCG CCT CCT CGG CCA GCT CCA CGT CCC GGA TCA-3′), forward primer-2 (5′-GCT CCA GGC GGT GCT TGT TCC TCA GCC TCT TCT CCT TCC TGA TCG TGG CAG GCG CCA CCA CGC TCT TCT GCC TGC TGC ACT TTG GAG TGA-3′), and reverse primer-2 (5′-TGC CTG GGC CAG AGG GCG CGG CCG CGA GAT CTC TGG GGA ACT CTT CCC TCT GGG GGC CGA TCA CTC CAA AGT GCA GCA GGC AGA AGA GCG-3′) containing BglII site at the 5′-end. The resulting amplified fragment was subcloned into the pY02 vector to generate pY02-preTNF. DNA fragments encoding non-cleavable wild-type human TNF (tm-wtTNFΔ1–12) (Fig. 2a), TNFR1-selective mutant TNF (tm-mutTNF-R1Δ1–12), and TNFR2-selective mutant TNF (tm-mutTNF-R2Δ1–12) which were generated by deleting amino acids 1–12 in the N-terminal part of TNF, were amplified by PCR from wtTNF, mutTNF-R1, and mutTNF-R2 respectively with the following primer pairs : forward primer-3 (5′-AGT GAT CGG CCC CCA GAG GGA AGC TTA GAT CTC TCT CTA ATC AGC CCT CTG GCC CAG GCA GTA GCC CAT GTT GTA GCA AAC CCT CAAG-3′) containing a BglII site at the 5′-end, and reverse primer-3 (5′-GGT TGG ATG TTC GTC CTC CGC GGC CGC CTA ACT AGT TCA CAG GGC AAT GAT CCC AAA GTA GAC CTG-3′) containing a NotI site at the 5′-end. These fragments were cloned into the pY02-preTNF vector. Then, fragments of tm-wtTNFΔ1–12, tm-mutTNF-R1Δ1–12, and tm-mutTNF-R2Δ1–12 were cloned between the SalI and NotI sites of the SIN vector construct, generating CSII-EF-tm-wtTNF-IRES-GFP, CSII-EF-tm-mutTNF-R1-IRES-GFP, and CSII-EF-tm-mutTNF-R2-IRES-GFP, respectively.

2.5. Preparation of lentiviral vectors

Lentiviral vectors were prepared as previously described [20,21]. In brief, 293T cells were transfected by the calcium phosphate method with three plasmids: packaging construct (pCAG-HIVgp), VSV-G and Rev expressing construct (pCMV-VSV-G-RSV-Rev) and

the SIN vector constructs (CSII-EF-tm-wtTNF-IRES-rhGFP, CSII-EF-tm-mutTNF-R1-IRES-rhGFP or CSII-EF-tm-mutTNF-R2-IRES-rhGFP) (Fig. 2b). Two days after transfection, the conditioned medium was collected and the virus was concentrated by ultracentrifugation at 50,000*g* for 2 h at 20 °C. The pelleted virus was re-suspended in Hank's balanced salt solution (GIBCO BRL, Paisley, UK). Vector titers were determined by measuring the infectivity of HeLaP4 cells with serial dilutions of vector stocks using flow cytometric analysis (FCM) for GFP-positive cells.

2.6. Creation of membrane-bound TNF expressing cells

To prepare tmTNF-expressing cells, DKO Mφ (1×10^3 cells/well) cells were transfected with each lentiviral vector (tm-wtTNF, tm-mutTNF-R1 or tm-mutTNF-R2) at a multiplicity of infection (MOI) of 160 in 96-well plates. Infected cells were cultured until reaching 1×10^7 cells. IRES-driven GFP-positive cells were single-cell-sorted by FACSVantage™ (BD Biosciences, Franklin Lakes, NJ), and cultured in conditioned medium from DKO Mφ cells. After blocking Fc receptors with anti-mouse CD16/32 (eBioscience, San Diego, CA), the expression of tmTNF on monoclonal cell lines was detected by staining with Phycoerythrin-conjugated anti-human TNF antibody (clone MAb11, eBioscience) at 0.5 μg/5×10^5 cells for 30 min on ice. Subsequently, the cells were washed with 1% FBS/PBS and re-suspended in 500 μl of 4% paraformaldehyde. GFP or phycoerythrin fluorescence was analyzed using FCM by FACSCalibur™. Monoclonal cell lines stably expressing tmTNF or its mutants and GFP (tmTNF-expressing Mφ, tm-wtTNF Mφ, tm-mutTNF-R1 Mφ, or tm-mutTNF-R2 Mφ) were used for the following experiments.

2.7. Measurement of receptor binding activity by FCM

To detect the binding of soluble human TNFR1 (shTNFR1) or TNFR2 (shTNFR2) to tmTNF on Mφ cell lines, shTNFR1- or shTNFR2-Fc chimera were labeled with R-phycoerythrin by Zenon™ Human IgG Labeling Kits (Invitrogen Corp.) according to the manufacturer's procedure. Briefly, 10 μl of shTNFR1- or shTNFR2-Fc chimera (250 μg/ml) (R&D systems) was incubated with 5 μl labeling reagent for 5 min at room temperature, and 5 μl blocking reagent was added to each reaction solution. After incubation for 5 min at room temperature, 4 μl each reaction solution was added to 5×10^5 cells/tube which were pretreated with mouse Fc block. After incubation for 30 min on ice, the cells were washed with 1% FBS/PBS, and then suspended in 500 μl of 0.4% paraformaldehyde.

3. Results and discussion

An understanding of the bioactivity of tmTNF is key to a better understanding of the overall function of TNF and TNF receptors. The relative contribution of signaling by tmTNF through the TNFR1 and TNFR2 receptors is unclear, as it is difficult to monitor the specific activation of these two receptors in response to tmTNF. To address this problem, we established macrophage cell lines expressing TNFR-selective mutant TNFs (tmTNF-R1 or tmTNF-R2) on the cell surface.

First, to assess the receptor selectivity of soluble mutTNF-R1 or R2 (sol-mutTNF-R1 or R2), which we previously created using a phage display system [18], we measured human TNFR1-mediated bioactivities of sol-mutTNFs on HEp-2 cells and human TNFR2-mediated bioactivities on hTNFR2/mFas-PA cells (Fig. 1a and Table 1). The binding affinity and kinetic parameters of these mutant TNFs for each TNF receptor were also measured using a Surface plasmon resonance assay (Fig. 1b and Table 1). We observed that both the bioactivity and binding affinity of sol-mutTNF-R1 for hTNFR1 were equivalent to those of sol-wtTNF, whereas the activity and affinity of sol-mut-TNF-R1 for hTNFR2 were decreased to less than 0.2% and 8%, respectively, of the values observed with sol-wtTNF. Although the bioactivity of sol-mutTNF-R2 mediated via hTNFR2 was only 16% of that of sol-wtTNF, the binding affinity of sol-mutTNF-R2 for human TNFR2 was about 1.5 times higher than that of sol-wtTNF. The bioactivity and binding affinity of sol-mutTNF-R2 for hTNFR1 were decreased to less than 0.1% and 3%, respectively, of the corresponding values for sol-wtTNF. Interestingly, the kinetic parameters, k_{on} and k_{off}, of the sol-mutTNFs for the TNF receptors tended to be higher than those of sol-wtTNF, indicating rapid association/dissociation interaction. From these data, we confirmed a significant TNFR-selectivity of sol-mutTNF-R1 and sol-mutTNF-R2. Therefore, we attempted to create the corresponding TNFR-selective tmTNFs using these sol-mutTNFs.

To express only tmTNF on the cell surface, the recombinant genes corresponding to each sol-TNF mutant, each encoding a protein with an additional twelve amino acid deletion from the N-terminus, were subcloned into lentiviral vectors (Fig. 2a and b). The resulting recombinant lentiviral vectors were transduced into $TNFR1^{-/-}R2^{-/-}$ macrophages (DKO Mφ). As previously reported, the deletion of the first 12 amino acids from the N-terminus of TNF, including the entire TACE cleavage site, leads to the expression of only the tmTNF form, and not the soluble form [15,22]. Since the SIN vector also comprises a GFP expression cassette, GFP expression was visible in all three cell lines: wtTNF-expressing DKO Mφ (tm-wtTNF Mφ), mutTNF-R1 expressing DKO Mφ (tm-mutTNF-R1 Mφ), and mutTNF-R2 expressing DKO Mφ (tm-mutTNF-R2 Mφ) (Fig. 2c). We next verified the expression of TNF on single sorted cells using FCM analysis. We observed significant expression of TNF on tm-wtTNF Mφ (Fig. 3a). The mean fluorescence intensity (MFI) of tm-mutTNF-R1 Mφ and tm-mutTNF-R2 Mφ was lower than that of tm-wtTNF Mφ (Fig. 3b). Since the expression level of GFP on tm-mutTNF-R1 Mφ and tm-mutTNF-R2 Mφ was lower than that on tm-wtTNF Mφ (Fig. 2c), the expression level of TNF on these cells might also be lower than that on tm-wtTNF Mφ.

Next, the affinity of each cell-surface expressed tmTNF for soluble TNF receptors was measured by FCM analysis (Fig. 4a), and receptor selectivity was estimated (Fig. 4b and c). We observed that both soluble TNFR1 and TNFR2 Fc chimeras bound to tm-wtTNF Mφ, although TNFR2 bound to tm-wtTNF Mφ with an affinity approximately twofold stronger than that of TNFR1 (Fig. 4b). Although the affinity of tm-mutTNF-R1 Mφ for TNFR1 was 50% that of tm-wtTNF Mφ, the affinity of tm-mutTNF-R1 Mφ for TNFR2 was greatly decreased and the ratio of selectivity of tm-mutTNF-R1 Mφ for TNFR1 over TNFR2 (R1/R2 of MFI) was approximately three times that of tm-wtTNF Mφ (Fig. 4b and c). Therefore, the expression of mutTNF-R1 on the cell surface as the tmTNF form demonstrates TNFR1 selectivity, as does its soluble form. On the other hand, the affinity of TNFR1 and TNFR2 for tm-mutTNF-R2 Mφ was weaker than their affinity for tm-wtTNF Mφ (Fig. 4a and b). Additionally, the ratio of selectivity of tm-mutTNF-R2 Mφ for TNFR1 over TNFR2 was similar to that of tm-wtTNF Mφ, indicating little selectivity for TNFR2 in contrast to what was observed for sol-mutTNF-R2 (Fig. 4c). We next evaluated the bioactivity of these tmTNFs via hTNFR2, by assessing the cytotoxicity of these tmTNFs on hTNFR2/mFas-PA cells, which express the hTNFR2/mFas chimeric receptor (Fig. 5). As previously reported, a cytotoxicity assay using hTNFR2/mFas-PA cells is a simple and highly sensitive assay system for determining TNFR2-mediated activity. DKO Mφ expressing each type of tmTNF (effector cell) were fixed with paraformaldehyde, and co-cultured with hTNFR2/mFas-PA cells (target cell). The viability of the target cells decreased significantly and in a dose-dependent manner

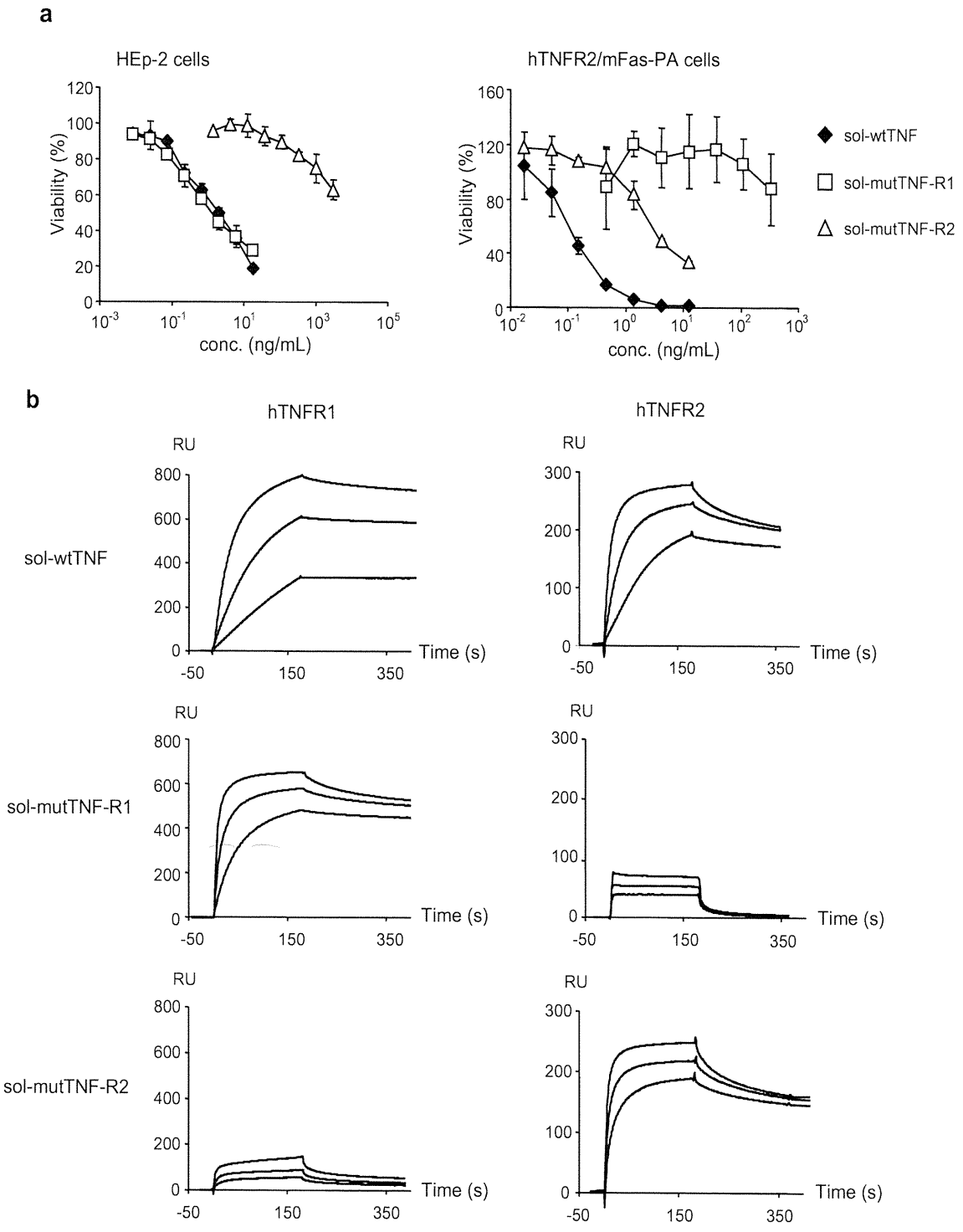

Fig. 1. Bioactivity and binding of sol-wtTNF, sol-mutTNF-R1, and sol-muTNF-R2 to TNFRs. (a) HEp-2 cells or hTNFR2/Fas-PA cells were used for measuring TNFR1-mediated or TNFR2-mediated bioactivity respectively. HEp-2 cells were cultured in serial dilutions of sol-wtTNF, sol-mutTNF-R1, and sol-mutTNF-R2 with 100 μg/ml cycloheximide for 18 h. hTNFR2/Fas-PA cells were also cultured in serial dilutions of sol-TNFs with 1 μg/ml cycloheximide for 48 h. Cell viability was determined using the methylene blue assay for HEp-2 cells, and the WST-8 assay for hTNFR2/Fas-PA cells. (b) The binding kinetics of sol-TNFs to immobilized TNFRs were analyzed using the surface plasmon resonance (SPR) technique. TNFRs were immobilized to a sensor chip CM5, which resulted in an increase of 3000–3500 resonance units (RU). The amount of protein bound to the surface was recorded in RU. Duplicate injections of 156.8, 52.3, or 17.4 nM sol-TNFs were passed over the immobilized TNFRs at a flow rate of 20 μl/min. The sensorgrams shown were normalized by subtracting the control surface sensorgram.

when exposed to an increasing *E*(effector)/*T*(target) cell ratio of tm-wtTNF Mφ compared to exposure to the control DKO Mφ. These results suggest that tmTNF induced death of these cells in a dose-dependent manner via signaling through the TNFR2/mFas chimera expressed on the target cell surface. The bioactivity of tm-mutTNF-R1 Mφ was lower than that of tm-wtTNF Mφ in

Table 1
Amino acid sequence, bioactivity, and kinetic parameters of mutTNFs.

Human TNFs	Amino acids sequence						Bioactivity EC50 (nM)		Binding property					
									TNFR1			TNFR2		
	29	31	32	145	146	147	HEp-2	hTNFR2/ mFas-PA	k_{on} $(M^{-1}\,S^{-1})^a$	k_{off} $(s^{-1})^b$	k_d $(nM)^c$	k_{on} $(M^{-1}\,S^{-1})^a$	k_{off} $(S^{-1})^b$	k_d $(nM)^c$
sol-wtTNF	L	R	R	A	E	S	1.9 (100%)	0.5 (100%)	2.1×10^5	1.4×10^{-4}	0.68 (100%)	1.1×10^6	7.8×10^{-4}	0.70 (100%)
sol-mutTNF-R1	K	A	G	A	S	T	1.5 (128%)	>300 (<0.2%)	6.5×10^5	4.7×10^{-4}	0.73 (93%)	5.8×10^6	522.0×10^{-4}	9.0 (8%)
sol-mutTNF-R2	L	R	R	R	E	T	>3000 (<0.1%)	3.1 (16%)	1.8×10^5	36.1×10^{-4}	20.2 (3%)	3.1×10^6	15.4×10^{-4}	0.49 (144%)

Kinetic parameters for each TNF were calculated by from the respective sensorgrams by BIA evaluation 3.0 software. Value in parenthesis shows the relative bioactivity or relative binding affinity (%).

[a] k_{on} is association kinetic constant.

[b] k_{off} is dissociation kinetic constant.

[c] k_d (equilibrium dissociation constant) denotes binding affinity.

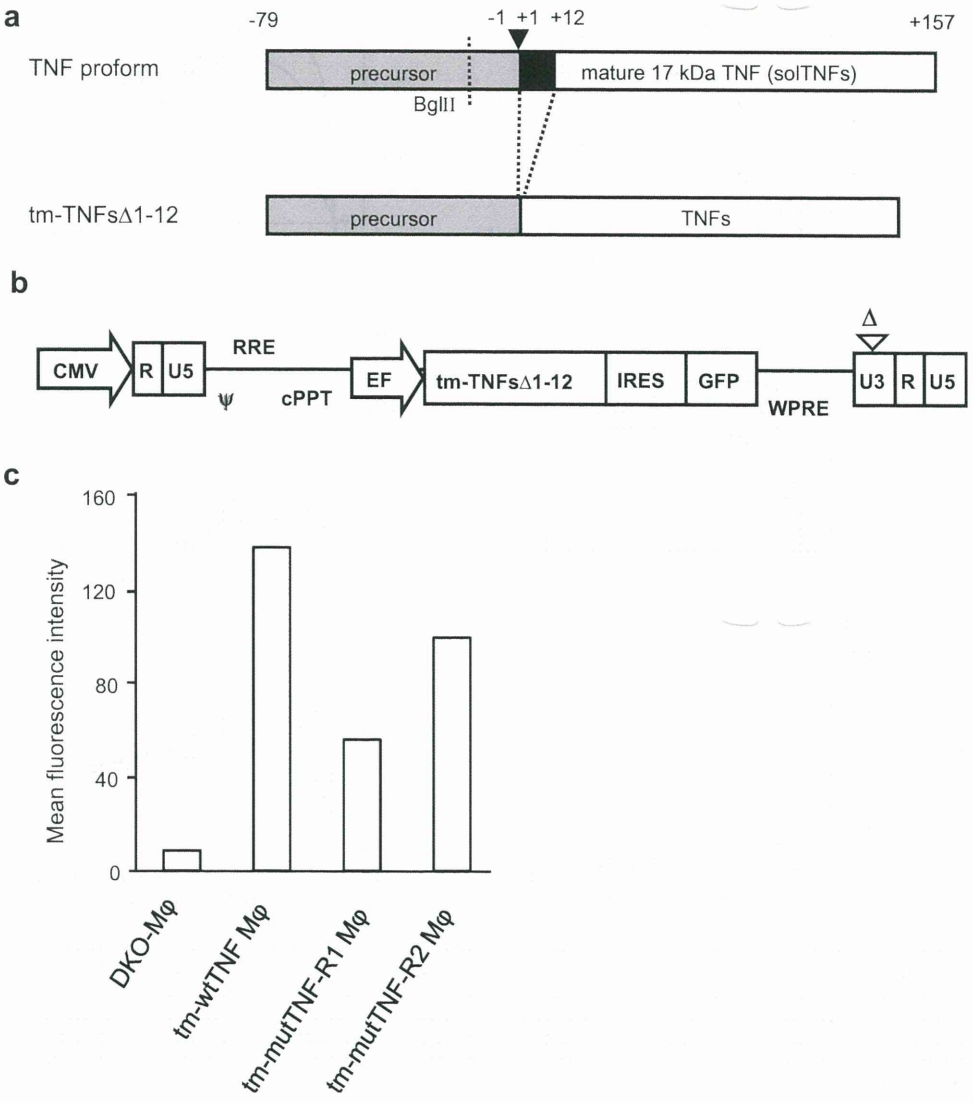

Fig. 2. Schematic representation of the tmTNF forms and the construction of the lentiviral vector. (a) Schematic representation of non-cleavable human TNFs (tm-TNFsΔ1–12). An inverted filled triangle shows the cleavage site. Closed bar, amino acids 1–12, indicates the deleted region. (b) Schematic representation of self-inactivating (SIN) LV plasmid (CSII-EF-tm-TNFsΔ1–12-IRES-GFP). CMV: cytomegalovirus promoter, ψ: packaging signal, RRE: rev responsive element, cPPT: central polypurine tract, IRES: Encephalomyocarditis virus internal ribosomal entry site, Bsd: Blasticidin, WPRE: woodchuck hepatitis virus posttranscriptional regulatory element. Δ: deletion of 133 bp in the U3 region of the 3′ long terminal repeat. (c) Expression of GFP on each cell was analyzed by FCM, and the mean fluorescence intensity of each cell is shown.

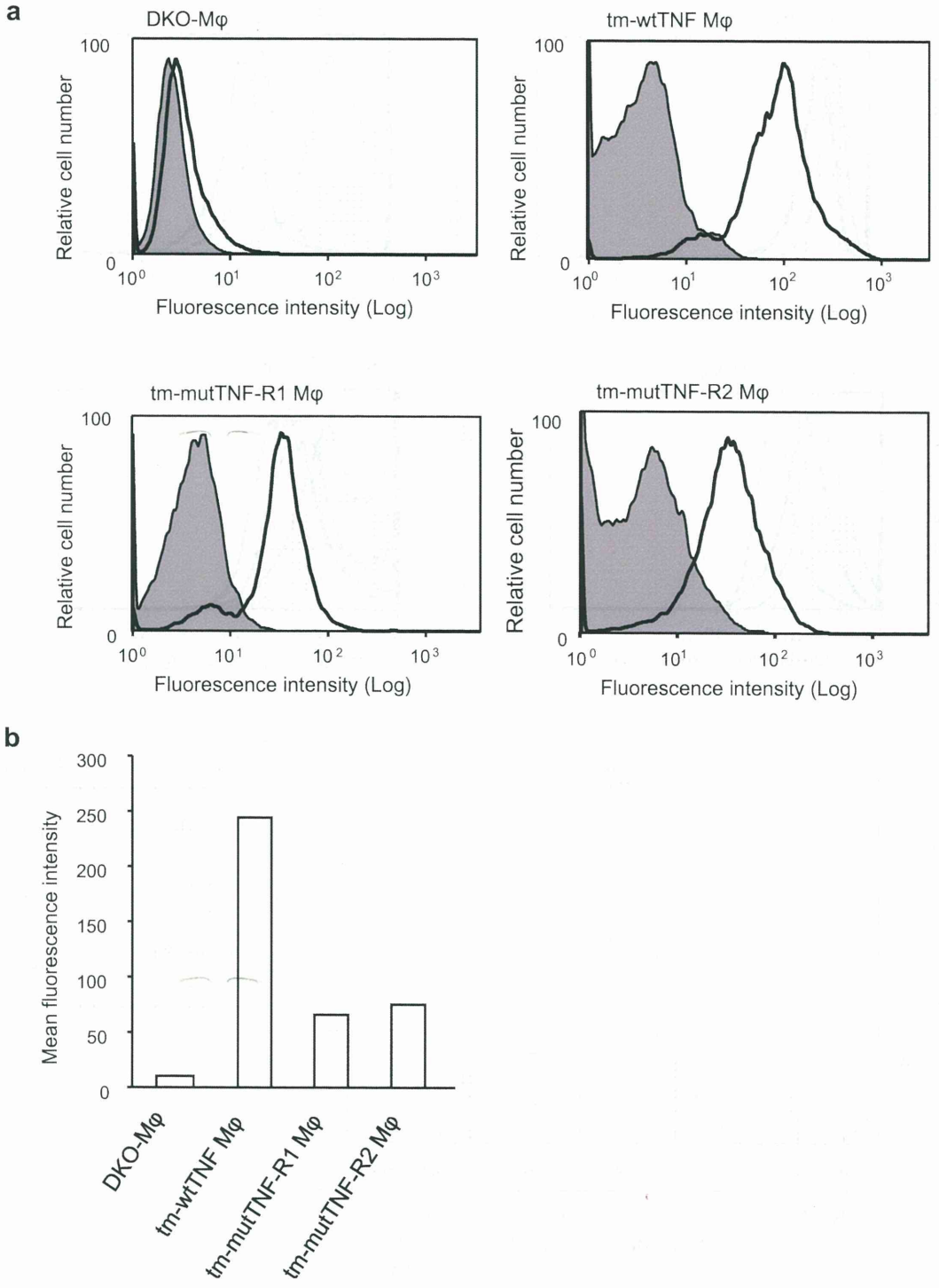

Fig. 3. The expression of TNF as the transmembrane form on tm-TNFs Mφ. (a) Expression of TNF on each cell was analyzed by FCM using PE-conjugated anti-hTNF monoclonal antibody (open histograms) or PE-conjugated isotype control antibody (shaded histograms). (b) The mean fluorescence intensity of each cell is shown.

this assay, which correlates with the results observed when studying its soluble form in Table 1. Interestingly, tm-mutTNF-R2 Mφ was more cytotoxic than tm-wtTNF Mφ, whereas the cytotoxicity of sol-mutTNF-R2 was only 16% of that of sol-wtTNF in this assay.

In this study, we have established the selectivity of tm-mutTNF-R1 Mφ for binding to TNFR1, although we need to measure the precise expression level of TNF in each cell. In addition, FCM analysis suggested that tm-mutTNF-R2 Mφ have a lower affinity for both TNFRs than do tm-wtTNF Mφ, and that they exhibit little selectivity

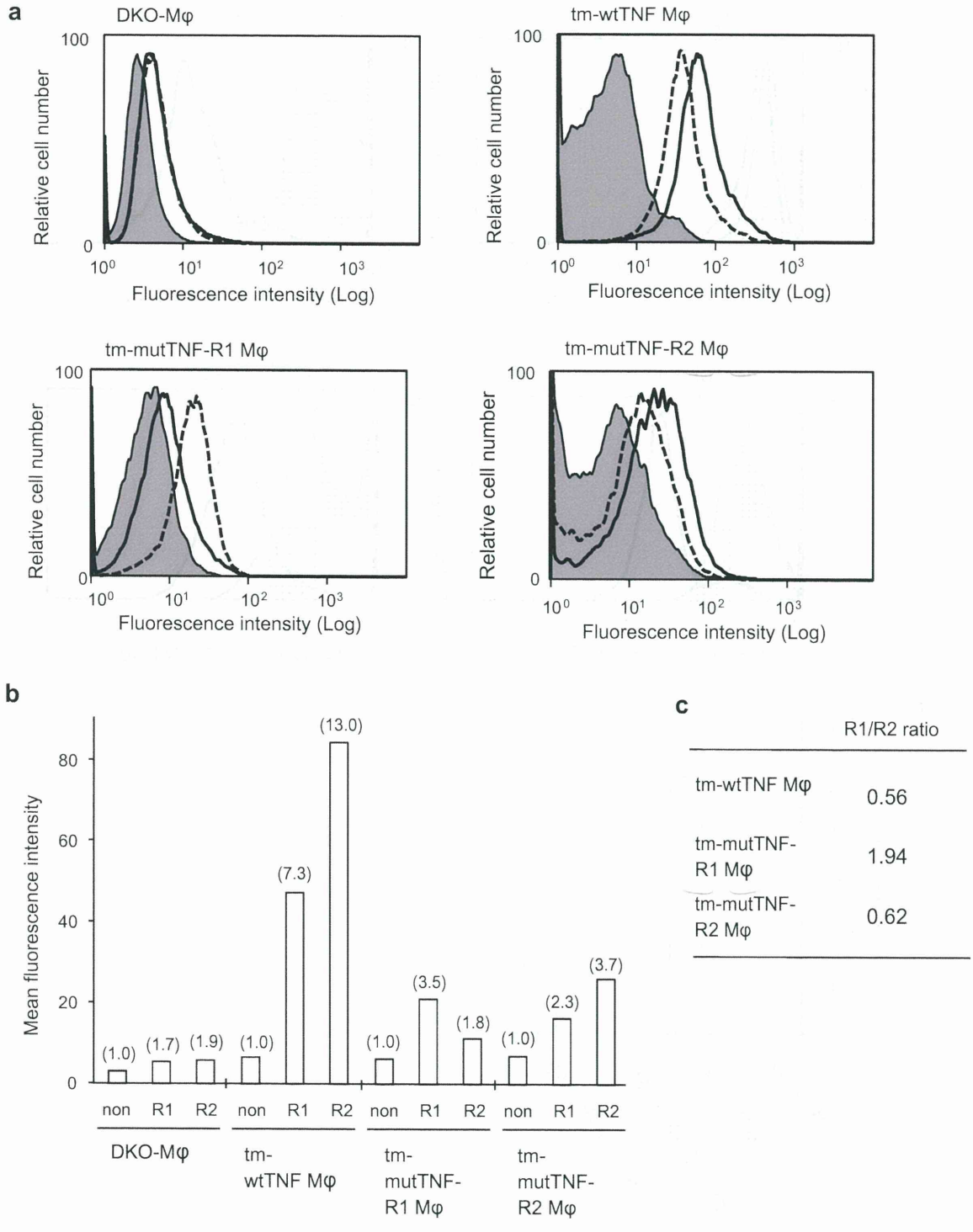

Fig. 4. The affinity of tm-TNFs Mφ for soluble TNF-receptors. (a) The binding of each tmTNF to solTNFR1 (dashed lines) or solTNFR2 (solid lines) was analyzed by FCM analysis. DKO Mφ, tm-wtTNF Mφ, tm-mutTNF-R1 Mφ, and tm-mutTNF-R2 Mφ were stained with solTNFR1- or solTNFR2-Fc chimera that was labeled with PE-conjugated Fab fragment of anti-human Fc antibody. Shaded histograms show non-stained cells. (b) Mean fluorescence intensity of each cells is shown. (c) Values in parenthesis indicate the relative intensity against non-treated cells in each cell line.

for TNFR2. In this report, we established macrophage cell lines expressing only tmTNF, and not solTNF, owing to the deletion of the first 12 amino acids (Δ1–12) of each TNF mutant. Although most studies have made use of the Δ1–12 TNF mutation for the investigation of tmTNF activity, the bioactivity of the resulting non-cleavable tmTNF is reported to be reduced compared to

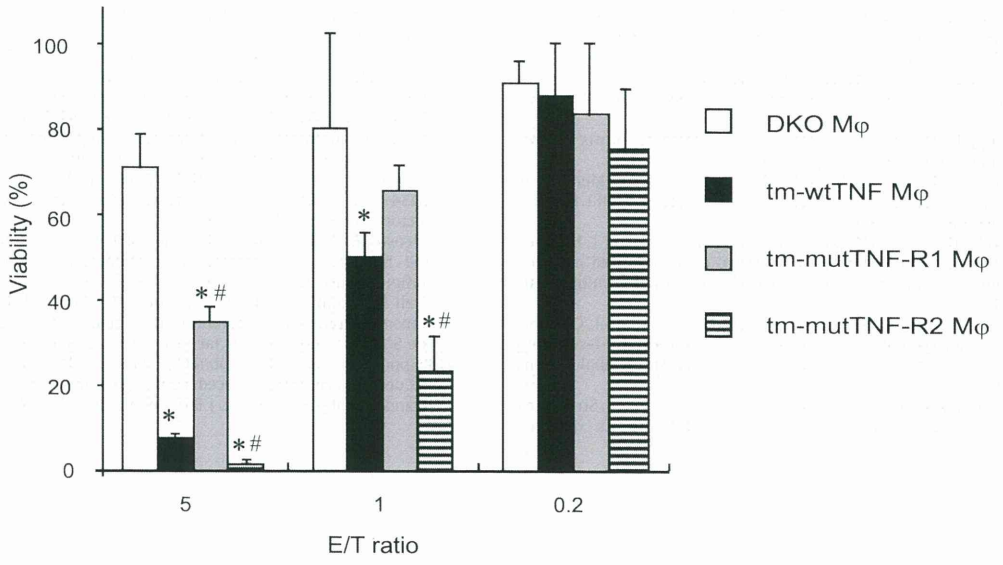

Fig. 5. tm-mutTNF-R2 Mφ induced death of hTNFR2/mFas-PA cells. hTNFR2/mFas-PA cells were co-incubated with paraformaldehyde-fixed DKO Mφ (open bars), tm-wtTNF Mφ (filled bards), tm-mutTNF-R1 Mφ (shaded bards), or tm-mutTNF-R2 Mφ (stiped bards) at an effector/target (E/T) ratio of 5:1, 1:1, or 0.2:1 in the presence of cycloheximide (1 μg/ml). After 48 h, cell viability was measured by the WST-8 Assay. Data were expressed as mean values ± SD of triplicate measurements and analyzed by one-way ANOVA (Dunnett's test). $^{*}p < 0.05$: compared to DKO Mφ, $^{\#}p < 0.05$: compared to tm-wtTNF Mφ.

wild-type tmTNF, whereas a tmTNF mutant containing a Δ1–9 K11E mutation exhibited normal cell-surface expression and a bioactivity similar to the wild-type [22]. Therefore, use of this latter deletion backbone may allow greater TNFR-selectivity in Mφ engineered to express tm-mutTNF-R2, and may generate superior TNFR-selective tmTNF-expressing cells.

As described earlier, tmTNF and solTNF have distinct roles or functions in normal and pathological conditions [8]. Furthermore, it is also believed that TNFR2 can only be fully activated by tmTNF [23]. Although the mechanisms underlying these effects are poorly understood, the half lives of the individual ligand/receptor complexes may contribute to the differential activity of tmTNF and solTNF [23]. Krippner-Heidenreich et al. reported that the dissociation rate constant of the cell surface binding of tmTNF to TNFR2 is much lower than that of the binding of solTNF to the same receptor, indicating that tmTNF dissociates much less readily from TNFR2 [24]. Thus, the bioactivity imparted by the interaction of the ligand/receptor pair is dependent upon various binding parameters (binding affinity, association or dissociation rate constant). We have shown here that tm-mutTNF-R2 Mφ exhibit greater cytotoxicity on hTNFR2/mFas-PA cells than do tm-wtTNF Mφ, whereas the cytotoxicity of sol-mutTNF-R2 was lower than that of sol-wtTNF. We assume that the dissociation rate constant of the binding of mutTNF-R2 to immobilized TNFR2 or TNFR2 on the cell surface might be reduced to a level similar to that of tm-wtTNF Mφ upon conversion of the soluble form to the transmembrane form. As such, the threefold higher association rate constant of the interaction of TNFR2 with sol-mutTNF-R2 than that of TNFR2 with sol-wtTNF (Table 1) might explain the strong bioactivity on hTNFR2/mFas-PA cells.

The affinity between a ligand and its receptor is determined by an equilibrium between the rates of association and dissociation, and is determined inherently. Therefore, expression of sol-mutTNFs with selectivity for each TNFR as the corresponding tmTNF forms on the cell surface, may alter the selectivity for the TNFRs. We plan to carry out more detailed analyses of the variant tmTNFs, such as measurement of their expression, their precise affinity for TNFR1 or R2, and their activity mediated through binding and signaling through TNFR1. Eventually, these tmTNFs, tm-mutTNF-R1 and R2 Mφ may prove useful for functional analysis or signal analysis of TNF receptors.

Acknowledgments

This study was supported in part by some Grants-in-Aid for Scientific Research from the Ministry of Education, Culture, Sports, Science and Technology of Japan, and in part by some Grants-in-Aid for Scientific Research from Japan Society for the Promotion of Science (JSPS). And this study was also supported in part by some Health Labour Sciences Research Grants from the Ministry of Health, Labor and Welfare of Japan, and in part by Health Sciences Research Grants for Research on Publicly Essential Drugs and Medical Devices from the Japan Health Sciences Foundation, in part by The Nagai Foundation Tokyo.

References

[1] Aggarwal BB. Signalling pathways of the TNF superfamily: a double-edged sword. Nat Rev Immunol 2003;3:745–56.
[2] Beutler B. Autoimmunity and apoptosis: the Crohn's connection. Immunity 2001;15:5–14.
[3] Feldmann M, Maini RN. Anti-TNF alpha therapy of rheumatoid arthritis: what have we learned? Annu Rev Immunol 2001;19:163–96.
[4] Feldmann M. Development of anti-TNF therapy for rheumatoid arthritis. Nat Rev Immunol 2002;2:364–71.
[5] Kriegler M, Perez C, DeFay K, Albert I, Lu SD. A novel form of TNF/cachectin is a cell surface cytotoxic transmembrane protein: ramifications for the complex physiology of TNF. Cell 1988;53:45–53.
[6] Tang P, Hung MC, Klostergaard J. Human pro-tumor necrosis factor is a homotrimer. Biochemistry 1996;35:8216–25.
[7] Black RA, Rauch CT, Kozlosky CJ, Peschon JJ, Slack JL, Wolfson MF, et al. A metalloproteinase disintegrin that releases tumour-necrosis factor-alpha from cells. Nature 1997;385:729–33.
[8] Ruuls SR, Hoek RM, Ngo VN, McNeil T, Lucian LA, Janatpour MJ, et al. Membrane-bound TNF supports secondary lymphoid organ structure but is subservient to secreted TNF in driving autoimmune inflammation. Immunity 2001;15:533–43.
[9] Mueller C, Corazza N, Trachsel-Loseth S, Eugster HP, Buhler-Jungo M, Brunner T, et al. Noncleavable transmembrane mouse tumor necrosis factor-alpha (TNFalpha) mediates effects distinct from those of wild-type TNFalpha in vitro and in vivo. J Biol Chem 1999;274:38112–8.
[10] Olleros ML, Guler R, Vesin D, Parapanov R, Marchal G, Martinez-Soria E, et al. Contribution of transmembrane tumor necrosis factor to host defense against Mycobacterium bovis bacillus Calmette-guerin and Mycobacterium tuberculosis infections. Am J Pathol 2005;166:1109–20.
[11] Saunders BM, Tran S, Ruuls S, Sedgwick JD, Briscoe H, Britton WJ. Transmembrane TNF is sufficient to initiate cell migration and granuloma formation and provide acute, but not long-term, control of Mycobacterium tuberculosis infection. J Immunol 2005;174:4852–9.

[12] Torres D, Janot L, Quesniaux VF, Grivennikov SI, Maillet I, Sedgwick JD. Membrane tumor necrosis factor confers partial protection to Listeria infection. Am J Pathol 2005;167:1677–87.
[13] Aggarwal BB, Eessalu TE, Hass PE. Characterization of receptors for human tumour necrosis factor and their regulation by gamma-interferon. Nature 1985;318:665–7.
[14] Micheau O, Tschopp J. Induction of TNF receptor I-mediated apoptosis via two sequential signaling complexes. Cell 2003;114:181–90.
[15] Perez C, Albert I, DeFay K, Zachariades N, Gooding L, Kriegler M. A nonsecretable cell surface mutant of tumor necrosis factor (TNF) kills by cell-to-cell contact. Cell 1990;63:251–8.
[16] Bryde S, Grunwald I, Hammer A, Krippner-Heidenreich A, Schiestel T, Brunner H, et al. Tumor necrosis factor (TNF)-functionalized nanostructured particles for the stimulation of membrane TNF-specific cell responses. Bioconjug Chem 2005;16:1459–67.
[17] Shibata H, Yoshioka Y, Ohkawa A, Minowa K, Mukai Y, Abe Y, et al. Creation and X-ray structure analysis of the tumor necrosis factor receptor-1-selective mutant of a tumor necrosis factor-alpha antagonist. J Biol Chem 2008;283:998–1007.
[18] Mukai Y, Shibata H, Nakamura T, Yoshioka Y, Abe Y, Nomura T, et al. Structure-function relationship of tumor necrosis factor (TNF) and its receptor interaction based on 3D structural analysis of a fully active TNFR1-selective TNF mutant. J Mol Biol 2009;385:1221–9.
[19] Abe Y, Yoshikawa T, Kamada H, Shibata H, Nomura T, Minowa K, et al. Simple and highly sensitive assay system for TNFR2-mediated soluble- and transmembrane-TNF activity. J Immunol Methods 2008;335:71–8.
[20] Katayama K, Wada K, Miyoshi H, Ohashi K, Tachibana M, Furuki R, et al. RNA interfering approach for clarifying the PPARgamma pathway using lentiviral vector expressing short hairpin RNA. FEBS Lett 2004;560:178–82.
[21] Miyoshi H, Smith KA, Mosier DE, Verma IM, Torbett BE. Transduction of human CD34+ cells that mediate long-term engraftment of NOD/SCID mice by HIV vectors. Science 1999;283:682–6.
[22] Decoster E, Vanhaesebroeck B, Vandenabeele P, Grooten J, Fiers W. Generation and biological characterization of membrane-bound, uncleavable murine tumor necrosis factor. J Biol Chem 1995;270:18473–8.
[23] Grell M, Douni E, Wajant H, Lohden M, Clauss M, Maxeiner B, et al. The transmembrane form of tumor necrosis factor is the prime activating ligand of the 80 kDa tumor necrosis factor receptor. Cell 1995;83:793–802.
[24] Krippner-Heidenreich A, Tubing F, Bryde S, Willi S, Zimmermann G, Scheurich P. Control of receptor-induced signaling complex formation by the kinetics of ligand/receptor interaction. J Biol Chem 2002;277:44155–63.

Biomaterials 32 (2011) 162–169

Contents lists available at ScienceDirect

Biomaterials

journal homepage: www.elsevier.com/locate/biomaterials

Development of an antibody proteomics system using a phage antibody library for efficient screening of biomarker proteins

Sunao Imai [a,1], Kazuya Nagano [a,1], Yasunobu Yoshida [a], Takayuki Okamura [a], Takuya Yamashita [a,b], Yasuhiro Abe [a], Tomoaki Yoshikawa [a,b], Yasuo Yoshioka [a,b,c], Haruhiko Kamada [a,c], Yohei Mukai [a,b], Shinsaku Nakagawa [b,c], Yasuo Tsutsumi [a,b,c], Shin-ichi Tsunoda [a,b,c,*]

[a] Laboratory of Biopharmaceutical Research, National Institute of Biomedical Innovation, 7-6-8 Saito-Asagi, Ibaraki, Osaka 567-0085, Japan
[b] Graduate School of Pharmaceutical Sciences, Osaka University, 1-6 Yamadaoka, Suita, Osaka 565-0871, Japan
[c] The Center of Advanced Medical Engineering and informatics, Osaka University, 1-6 Yamadaoka, Suita, Osaka 565-0871, Japan

ARTICLE INFO

Article history:
Received 27 August 2010
Accepted 14 September 2010
Available online 8 October 2010

Keywords:
Protein
Image analysis
Immunochemistry
Molecular biology
Antibody
Cancer

ABSTRACT

Proteomics-based analysis is currently the most promising approach for identifying biomarker proteins for use in drug development. However, many candidate biomarker proteins that are over- or under-expressed in diseased tissues are found by such a procedure. Thus, establishment of an efficient method for screening and validating the more valuable targets is urgently required. Here, we describe the development of an "antibody proteomics system" that facilitates the screening of biomarker proteins from many candidates by rapid preparation of cross-reacting antibodies using phage antibody library technology. Using two-dimensional differential in-gel electrophoresis analysis, 16 over-expressed proteins from breast cancer cells were identified. Specifically, proteins were recovered from the gel pieces and a portion of each sample was used for mass spectrometry analysis. The remainder was immobilized onto a nitrocellulose membrane for antibody-expressing phage enrichment and selection. Using this procedure, antibody-expressing phages against each protein were successfully isolated within two weeks. The expression profiles of the identified proteins were then acquired by immunostaining of breast tumor tissue microarrays with the antibody-expressing phages. Using this approach, expression of Eph receptor A10, TRAIL-R2 and Cytokeratin 8 in breast tumor tissues were successfully validated.

These results demonstrate the antibody proteomics system is an efficient method for screening tumor-related biomarker proteins.

1. Introduction

Proteomics-based analysis is the most promising approach for identifying tumor-related biomarker proteins used in the drug development process [1–3]. The technological development of proteomics to seek and identify differentially expressed proteins in disease samples is expanding rapidly. However, in spite of the identification of many candidate biomarkers, the number of biomarker proteins successfully applied to drug development has been limited. The main difficulty is the lack of a methodology to comprehensively analyze the expression or function of many candidate proteins and to efficiently select potential biomarker proteins of interest. To circumvent this problem, an improved technology to efficiently screen the truly valuable proteins from a large number of candidates is desirable.

Monoclonal antibodies are extremely useful tools for the functional and distributional analysis of proteins [4–6]. For example, they can be applied to the specific detection and study of proteins through various techniques including ELISA, Western blotting, fluorescent imaging and tissue microarray analysis (TMA). Of all these techniques, TMA is particularly valuable because it enables the analysis of clinical expression profiles of antigens from many clinical samples [7–11]. However, the common hybridoma-based antibody production is a laborious and time-consuming method. Thus, it is impractical to create antibodies against many differentially expressed proteins identified by proteomics technologies, such as two-dimensional differential in-gel electrophoresis (2D-DIGE) [12–15]. Furthermore, a relatively large amount of antigen (several milligrams) is necessary to produce an antibody (i.e., immunization of animals or screening of positive clones). The

* Corresponding author. Laboratory of Biopharmaceutical Research, National Institute of Biomedical Innovation, 7-6-8 Saito-Asagi, Ibaraki, Osaka 567-0085, Japan. Tel.: +81 72 641 9814; fax: +81 72 641 9817.
E-mail address: tsunoda@nibio.go.jp (S.-i. Tsunoda).
[1] These authors contributed equally to the work.

0142-9612/$ – see front matter © 2010 Elsevier Ltd. All rights reserved.
doi:10.1016/j.biomaterials.2010.09.030

production of protein on this scale often requires engineering the corresponding gene for heterologous expression, which may require some time to optimize. In this respect, phage antibody library technology is able to construct a large repertoire protein or peptide consisting of hundreds of millions of molecules. Monoclonal antibodies against target antigens are then rapidly obtained from the phage libraries displaying single chain fragment variable (scFv) antibodies *in vitro* [16–21].

However, the amount of protein in spots detected by 2D-DIGE analysis is generally very small (hundreds of nanograms). Therefore, a technology for generating monoclonal antibodies from such small amounts of antigen needs to be developed. There are no reports that describe the successful isolation of antibodies against small amounts of proteins obtained from differential proteome analysis.

Here, we report the establishment of a method for the efficient isolation of scFv antibody-expressing phages from a small amount of protein antigen prepared *via* 2D-DIGE spots using a high quality non-immune mouse scFv phage library [22]. We also describe an efficient method for screening and validating tumor-related biomarker proteins of interest from a number of differentially expressed proteins by expression profiling using TMA and scFv antibody-expressing phages.

2. Materials and methods

2.1. Non-immune mouse scFv phage library

Construction of the improved non-immune murine scFv phage library has been described previously [22]. The phage library was prepared from a TG1 glycerol stock containing the scFv gene library.

2.2. Affinity panning using BIAcore® and nitrocellulose membrane

Three different amounts (5000 ng, 50 ng or 0.5 ng) of KDR-Fc chimera (R&D systems Inc., Minneapolis, MN) or a portion of the proteins (1–5 ng) extracted from 2D-DIGE spots were immobilized on a BIAcore sensor chip CM3® (BIAcore, Uppsala, Sweden) or on a nitrocellulose membrane. BIAcore-based panning has been described previously [22]. Membrane-based panning was performed using the Bio-Dot Microfiltration Apparatus (Bio-Rad Laboratories, Hercules, CA). The membrane was incubated with blocking solution (10% skimmed milk, 25% glycerol) for 2 h and then washed twice with 0.1% TBST (Tris-buffered saline containing 0.1% Tween 20). The model phage library (anti-KDR scFv antibody-expressing phages: wild type phage = 1: 100) or the non-immune scFv phage library was pre-incubated with 90% blocking solution at 4 °C for 1 h and then applied to each well. After 2–3 h incubation, the apparatus was washed ten times with TBST. Bound scFv antibody-expressing phages were then eluted with 100 mM triethylamine. The eluted phages were incubated in log phase *E. coli* TG1 cells and glycerol-stocks prepared for further repeat panning cycles. Phage titer was measured by counting the number of infected colony cells on Petrifilm (3M Co., St. Paul, MN).

2.3. Colony direct PCR

After the panning, colonies of phage-infected TG1 were picked up at random as PCR templates. The gene inserts of 16 clones were amplified by PCR using the following primers: primer-156 (5′-CAACGTGAAAAAATTATTATTCGC-3′) and primer-158 (5′-GTAAATGA ATTTTCTGTATGAGG-3′), which anneal to the sequences of pCANTAB5E phagemid vector (GE Healthcare Biosciences AB, Uppsala, Sweden). The size of insert DNA sequence was analyzed by agarose gel electrophoresis.

2.4. Cell lines

Human mammary gland cell line 184A1 (American Type Culture Collection; ATCC, Manassas, VA) was maintained by MEGM Bullet Kit (Takara Bio, Shiga, JAPAN). Mammary gland-derived breast cancer cell line SKBR3 (ATCC) was maintained in McCoy's 5a plus 10% FBS. All cells were grown at 37 °C in a humidified incubator with 5% CO_2.

2.5. 2D-DIGE analysis

Cell lysates were prepared from human mammary gland cell line 184A1 and mammary gland-derived breast cancer cell line SKBR3, and then solubilized with 7 M urea, 2 M thiourea, 4% CHAPS and 10 mM Tris–HCl (pH 8.5). The lysates were labeled at the ratio 50 μg protein: 400 pmol Cy3 or Cy5 protein labeling dye (GE Healthcare Biosciences AB) in dimethylformamide according to the manufacture's protocol. For first dimension separation, the labeled samples (each 50 μg) were combined and mixed with rehydration buffer (7 M urea, 2 M thiourea, 4% CHAPS, 2% DTT, 2% Pharmalyte (GE Healthcare Biosciences AB)) and applied to a 24-cm immobilized pH gradient gel strip (IPG-strip pH 5–6 NL). The samples for the spot-picking gel were prepared without labelling by Cy-dyes. For the second dimension separation, the IPG-strips were applied to SDS-PAGE gels (10% polyacrylamide and 2.7% N,N′-diallyltartardiamide gels). After electrophoresis, the gels were scanned with a laser fluoroimager (Typhoon Trio, GE Healthcare Biosciences AB). The spot-picking gel was scanned after staining with Flamingo solution (Bio-Rad). Quantitative analysis of protein spots was carried out with Decyder-DIA software (GE Healthcare Biosciences AB). For the antigen spots of interest, spots of 1 × 1 mm in size were picked using an Ettan Spot Picker (GE Healthcare Biosciences AB). Proteins were extracted by solubilizing the picked gel pieces using 88 mM sodium periodide. Protein volumes were determined by BSA standard in Colloid Gold Total Protein staining (Bio-Rad).

2.6. In-gel tryptic digestion

Spots of 1 mm × 1 mm in size were picked using an Ettan Spot Picker and digested with trypsin as described below. The gel pieces were then destained with 50% acetonitrile/50 mM NH_4HCO_3 for 20 min twice, dehydrated with 75% acetonitrile for 20 min, and then dried using a centrifugal concentrator. Next, 5 μl of 20 μl/ml trypsin (Promega, Madison, WI) solution was added to each gel piece and incubated for 16 h at 37 °C. Three solutions were used to extract the resulting peptide mixtures from the gel pieces. First, 50 μl of 50% (v/v) acetonitrile in 1% (v/v) aqueous trifluoroacetic acid (TFA) was added to the gel pieces, which were then sonicated for 5 min. Next, we collected the solution and added 80% (v/v) acetonitrile in 0.2% TFA. Finally, 100% acetonitrile was added for the last extraction. The peptides were dried and then resuspended in 10 μl of 0.1% TFA before being cleaned using ZipTip^{TM} μC_{18} pipette tips (Millipore, Billerica, MA). The tips were wetted with three washes in 50% acetonitrile and equilibrated with three washes in 0.1% TFA, then the peptides were aspirated 10 times to ensure binding to the column. The column and peptides were washed three times in 0.1% TFA before being eluted in 1 μl of 80% acetonitrile/0.2% TFA.

2.7. Mass spectrometry (MS) and database search

The tryptic digests (0.6 μl) were mixed with 0.6 μl α-cyano-4-hydroxy-trans-cinnamic acid saturated in a 0.1% TFA and acetonitrile solution (1:1vol/vol). Each mixture was deposited onto a well of a 96-well target plate and then analyzed by matrix-assisted laser desorption ionization time-of-flight mass spectrometry (MALDI-TOF/MS; autoflexII, Bruker Daltonics, Billerica, WI) in the Reflectron mode. The mass axis was adjusted with calibration peptide (BRUKER DALTNICS) peaks (M/z 1047.19, 1296.68, or 2465.19) as lock masses. Bioinformatic databases were searched to identify the proteins based on the tryptic fragment sizes. The Mascot search engine (http://www.matrixscience.com) was initially used to query the entire theoretical tryptic peptide as well as SwissProt (http://www.expasy.org/, a public domain database provided by the Swiss Institute of Bioinformatics, Geneva, Switzerland). The search query assumed the following: (i) the peptides were monoisotopic (ii) methionine residues may be oxidized (iii) all cysteines are modified with iodoacetamide.

2.8. Phage ELISA using nitrocellulose membrane

Phage ELISA using scFv antibody-expressing phages was performed as previously described [22]. Briefly, phage-infected TG1 clones were picked, monocloned in a Bio-Dot Microfiltration Apparatus and scFv antibody-expressing phages propagated. The supernatants containing scFv antibody-expressing phages were incubated with immobilized proteins (~1 ng) extracted from 2D-DIGE spots. scFv antibody-expressing phages bound to 2D-DIGE spots were visualized using HRP-conjugated anti-M13 monoclonal antibody (GE Healthcare Biosciences AB).

2.9. Immunohistochemical staining using scFv antibody-expressing phages

Human breast cancer and normal TMA (Super Bio Chips, Seoul, South Korea & Biomax, Rockville, MD) were deparaffinated in xylene and rehydrated in a graded series of ethanol. Heat-induced epitope retrieval was performed in while keeping Target Retrieval Solution pH 9 (Dako, Glostrup, Denmark) temperature following the manufacturer's instructions. Heat-induced epitope retrieval was performed while maintaining the Target Retrieval Solution pH 9 (Dako) at the desired temperature according to the manufacturer's instructions. After heat-induced epitope retrieval treatment, endogenous peroxidase was blocked with 0.3% H_2O_2 in TBS for 5 min followed by washing twice in TBS. TMA were incubated with 5% BSA blocking solution for 15 min. The slides were then incubated with the primary scFv antibody-expressing phages (10^{12} CFU/ml) for 60 min. After washing three times with 0.05% TBST, each series of sections was incubated for 30 min with ENVISION + Dual Link (Dako), washed three times in TBST. The reaction products were rinsed twice with TBST, and then developed in liquid 3,3′-diaminobenzidine (Dako) for 3 min. After the development, sections were washed twice with distilled water, lightly